causes such as osteoarthritis (34–36). Moreover, RA synovial fluids induced a greater scattering of cells than did osteoarthritis synovial fluids (34). These reports indicate that HGF may play some role in RA. Because HGF is an angiogenesis factor, it might promote joint inflammation. In contrast, considering its immunosuppressive effect, HGF might suppress the development of Ag-induced arthritis. To date, it has not been studied whether HGF would suppress immune-mediated arthritis.

To determine the effect of HGF on autoimmune arthritis, we delivered HGF to mice and examined the effect on collagen-induced arthritis (CIA). We immunized mice with type II collagen (CII) and induced experimental arthritis. HGF was applied s.c. and delivered by gelatin-coupled controlled release to achieve a sustained and effective delivery. The T cell response to CII was analyzed in vitro, and arthritis was examined in vivo. HGF suppressed CII-induced T cell priming in the spleen and diminished the severity and incidence of arthritis with up-regulation of IL-10 and suppression of IL-17.

Materials and Methods

Mice

Male BALB/c mice (aged 6 wk) and DBA/1 mice (aged 7 wk) were obtained from Charles River Laboratories Japan. They were maintained under conventional animal housing conditions in a specific pathogen-free setting. All of the animal experiments conducted in this study were approved by the Animal Research Ethics Board of the Department of Allergy and Rheumatology, University of Tokyo, Tokyo, Japan.

ELISA

Concentrations of mouse IL-4, IL-10, IL-12p70, IFN-γ (BD Pharmingen), IL-23 (eBioscience), and CII-specific IgG (Chondrex) were measured using an ELISA kit following the manufacturer's protocol. Concentrations of human HGF in the sera were measured using an IMMUNIS HGF enzyme immunoassay kit (Institute of Immunology, Tokyo, Japan). CII-specific IgG2a was measured with ELISA grade type II collagen (Chondrex) for capture and HRP-conjugated anti-mouse IgG2a Ab (BD Pharmingen) for detection. The average concentration of the sera from the control mice on day 40 was defined as 1000 ELISA unit (EU). Mouse IL-17 was measured by ELISA using purified rat anti-mouse IL-17 mAb for capture and biotinylated rat anti-mouse IL-17 mAb for detection (BD Pharmingen). The titers of samples for IL-17 were calculated by comparison with internal standards. On day 10 after sensitization, lymph node (LN) cells were obtained from mice sensitized with CII/CFA and restimulated in vitro with CII (10 μg/ml) for 4 days. The average concentration in the supernatants was defined as 1000 EU. Cell proliferation was measured by BrdU incorporation using a BrdU cell proliferation ELISA kit (Roche). The data were analyzed with Microplate Manager III, version 1.45 (Bio-Rad).

Preparation of gelatin microspheres incorporating HGF

Acidic gelatin hydrogel microspheres were prepared from gelatin with an isoelectric point of 5.0 (Nitta Gelatin) as reported previously (37, 38). The solution (5 mg/ml) of recombinant human HGF (rhHGF) (1, 2) was dropped onto 2 mg of gelatin microspheres and left at 37°C for 1 h so that the HGF could impregnate the microspheres. In a previous study, we confirmed that when this gelatin/rhHGF complex was s.c. injected into mice a controlled release of HGF was achieved based on hydrogel degradation and that the degradation occurred over 10 days (37). In the present study, gelatin or gelatin/rhHGF were diluted in 100 μl of PBS and then injected into mice.

Conditions for cell culture

Throughout the present study complete DMEM was used as the medium for cell incubation as we previously reported (24, 39). Cells were incubated in a 96-well, flat-bottom, microtiter assay plate in an incubator (37°C with 5% CO2 and 90% humidity) for given periods.

Preparation of single cell suspensions of spleen and lymph node cells

Single cell suspensions of spleens and femoral lymph nodes were prepared as in previous reports (39).

Purification of mouse splenic $CD4^+$ T cells and DCs

Mouse splenic $CD4^+$ T cells were negatively selected using an anti-mouse $CD4^+$ T cell isolation kit (Miltenyi Biotec). Mouse splenic DCs were positively selected using anti-mouse CD11c colloidal superparamagnetic microbeads (Miltenyi Biotec) as reported previously (24, 39–41). The purity of $CD4^+$ and $CD11c^+$ cells, confirmed by flow cytometry, was >95% and >85%, respectively.

Protocol for OVA/alum-induced immune responses

BALB/c mice were sensitized with 2 μg of OVA (Sigma-Aldrich) in 2 mg of alum (Serva) on day 0 as reported previously (24, 39). Then, a few hours after the OVA/alum injection mice received a single s.c. injection of gelatin (2 mg) or a gelatin/rhHGF complex (2 mg and 100 μg, respectively) in the dorsal skin. On day 10, spleen cells from each group of mice were collected and then restimulated in vitro with OVA. After 3 days of incubation with OVA at several concentrations, spleen cell proliferation was measured based on BrdU incorporation. After 4 days of incubation with OVA (100 μg/ml), cytokine concentrations in the supernatants were measured. $CD4^+$ T cells (1×10^6 cells/ml) were also negatively selected and then stimulated with PMA (1 ng/ml; Sigma-Aldrich) and ionomycin (0.1 μg/ml). After 2 days of incubation, IL-10 concentrations in the supernatants were measured.

Induction of CIA

CIA was induced as reported previously (42). In brief, CII (2 mg/ml in 0.05 M acetic acid) was emulsified with an equal volume of CFA (4 mg/ml; Chondrex). Mice were injected s.c. ~1–2 cm from the base of the tail with 100 μl of the emulsion on day 0. On day 21, the mice received a booster injection of the CII/IFA emulsion s.c. around the base of the tail. Mice also received s.c. injections of gelatin (2 mg) or gelatin/rhHGF (100 μg) complex diluted in 100 μl of PBS on day 0 and every 10 days thereafter. The development of arthritis was assessed by inspection on day 25 and then every 2 to 3 days. The clinical severity of arthritis in each paw was quantified according to a graded scale from 0 to 4 as follows: 0, no swelling; 1, swelling in one digit or mild edema; 2, moderate swelling affecting several digits; 3, severe swelling affecting most digits; and 4, the most severe swelling and/or ankylosis (42). A mean arthritis score was determined by summing the scores of all joints of all mice and dividing the result by the total number of mice in the group.

Histologic examination and ex vivo examination

Mice were killed on day 40 and the joints of the more severely swollen hind paw were obtained. Histologic examination of the joints was performed as reported previously (42). The pathologic condition was scored by two blinded examiners from the Sapporo General Pathology Institute (Sapporo, Japan) in four categories: cartilage, cellularity, pannus, and bone erosion. Each category was graded from 0 to 4 as follows: 0, normal; 1, minimal; 2, mild; 3, moderate; and 4, marked.

Protocol for ex vivo experiments in the CII-induced immune responses

CIA was induced as described above. To examine the effect of HGF on immunocytes, a single cell suspension of spleen or femoral LN was prepared and cell responses (5×10^6 cells/ml) to in vitro CII restimulation (10 μg/ml) were examined on days 10, 20, and 40. To examine the effect of HGF on DCs, splenic DCs were also positively selected from each group of mice on days 10, 20, and 40, and the production of cytokines by DCs (1×10^6 cells/ml) after LPS (1 μg/ml) stimulation for 2 days was examined. To examine the effect of DCs on $CD4^+$ T cells, in some experiments, DCs were cocultured with $CD4^+$ T cells with CII in the medium. For analysis of the Ag-presenting capacity of DCs after mitomycin C treatment (10 μg/ml for 35 min at 37°C) to inhibit cell proliferation of DCs themselves, DCs (1×10^5 cells/ml) and splenic $CD4^+$ T cells (1×10^6 cells/ml) from CII/CFA-sensitized control mice on day 10 were cocultured in the presence of CII (3 μg/ml). After 3 days of coculture, cell proliferation was measured by BrdU incorporation. For analysis of the effect of DCs on cytokine production by $CD4^+$ T cells, DCs from each group of mice and splenic $CD4^+$ T cells were cocultured with CII (10 μg/ml) in the medium. After 4 days of coculture, we examined cytokine production by $CD4^+$ T cells. We also examined the effect of HGF on the cytokine profile of $CD4^+$ T cells. $CD4^+$ T cells purified from each group of mice on days 10, 20, and 40 were stimulated with PMA and ionomycin as described above. Cytokine concentrations in the supernatants were measured after the indicated duration of incubation. To examine the effect of HGF in the presence of Ag on Ag-induced T cell activation, spleen cells (5×10^6 cells/ml) obtained

Table I. *Time course of HGF concentration in the sera (pg/ml)*[a]

Hours or Days after Injection	4 h	Day 1	Day 2	Day 4
HGF protein				
HGF (10 μg)	ND[b]	ND	ND	ND
HGF (100 μg)	1658 ± 447	216 ± 71	ND	ND
Gelatin/rhHGF complex				
HGF (0 μg)	ND	ND	ND	ND
HGF (100 μg)	801 ± 117	188 ± 34	174 ± 174	ND

[a] Data are the mean ± SEM from three to four animals per group.
[b] Not detected.

from CII/CFA-sensitized mice on day 10 were restimulated with CII (10 μg/ml) in the presence or absence of rhHGF at several concentrations. After 3 to 4 days of incubation, cytokine production was measured.

Flow cytometry

Expression of surface molecule on DCs obtained from each group of mice on day 10 was examined as reported previously (43) by flow cytometry (EPICS XL System II; Beckman Coulter). We also examined the expression of CD25 and Foxp3 in $CD4^+$ T cells on days 10, 20, and 40. Staining of spleen or LN cells with anti-mouse CD4, CD25, and Foxp3 Abs was conducted following the manufacturer's protocol. In brief, first the cells were stained with allophycocyanin-conjugated anti-mouse CD4 Ab and FITC anti-mouse CD25 Ab (BD PharMingen). Then, intracellular Foxp3 staining was conducted using anti-mouse Foxp3 Ab and fixation/permeabilization solution and permeabilization buffer contained in a mouse regulatory T cell staining kit (eBioscience). Then stained cells were analyzed by flow cytometry (EPICS Elite; Beckman Coulter).

RT-PCR

mRNA was extracted from $CD4^+$ T cells by the acid-guanidium phenol chloroform method using Isogen (Nippon Gene). Then, RT-PCR was conducted as reported previously (39). PCR for GATA-3 consisted of 1 min of denaturation at 94°C, 1 min of annealing at 60°C, and 1 min of extension at 72°C for 26 cycles. PCR for β-actin consisted of 1 min of denaturation at 94°C, 1 min of annealing at 61°C, and 1 min of extension at 72°C for 18 cycles. The sense primer for the transcription factor GATA-3 was 5′-TCT GGAGGAGGAAACGCTAATGG-3′ and the antisense primer was 5′-GAACTCTTCGCACACTTGGAGACTC-3′. The sense primer for β-actin was 5′-TGGAATCCTGTGGCATCCATGAAAC-3′ and the antisense primer was 5′-TAAAACGCAGCTCAGTAACAGTCCG-3′. PCR products were electrophoresed in a 3% agarose gel, and the results were visualized by ethidium bromide staining.

Statistical analysis

Values are expressed as the mean ± SEM. The Mann-Whitney *U* test was used to analyze the clinical scores and histologic findings. The unpaired *t* test was used to analyze the other results. Values of $p < 0.05$ were considered to be significant.

Results

HGF significantly suppresses T cell priming induced by OVA/alum

Generally, exogenously administered HGF protein delivered by i.v. injection vanishes from organs within several hours (44). So, to achieve efficient delivery of HGF we adopted biodegradable gelatin hydrogels as a carrier for the CIA model and delivered the HGF/gelatin complex by s.c. injection (37). First, we examined the time course of HGF concentration in sera after s.c. injection of HGF protein, gelatin, or gelatin/rhHGF complex. We confirmed that the more sustained release of HGF was achieved by s.c. injection of gelatin/rhHGF complex compared with the injection of HGF protein alone (Table I). Then, we examined the effect of this gelatin/rhHGF complex (designated HGF in figures) on OVA-induced immune responses. Spleen cells obtained from the mice

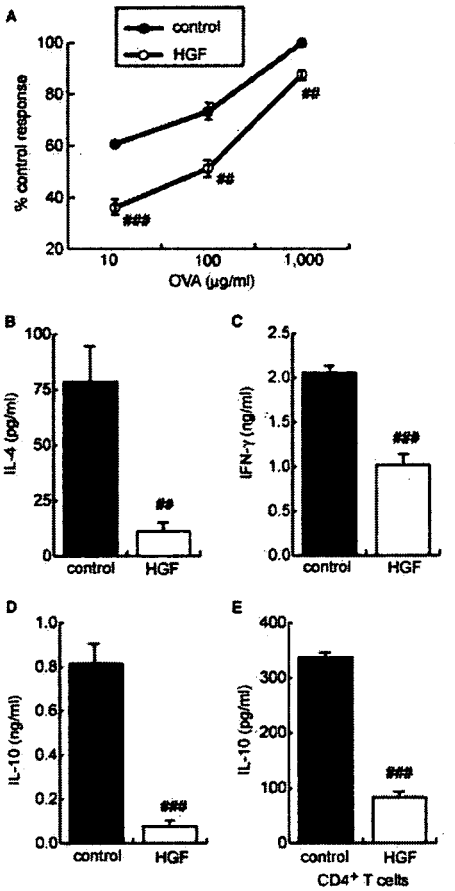

FIGURE 1. Controlled release of HGF in vivo potently suppresses T cell priming with OVA/alum. BALB/c male mice were sensitized with OVA/alum and a few hours later received a s.c. injection of gelatin (2 mg) (control mice) or gelatin/rhHGF (100 μg) complex (HGF) on day 0. On day 10, spleen cells were obtained from each group of mice. *A–E*, Spleen cell responses (2.5×10^6 cells/ml) to OVA restimulation in vitro were examined. *A*, Cell proliferation was measured after 3 days of incubation with the indicated concentrations of OVA. Data are expressed as a percentage of the response compared with that of spleen cells from control mice at OVA (1000 μg/ml). *B–D*, Production of IL-4 (*B*) and IFN-γ (*C*) as well as IL-10 (*D*) was measured by ELISA after 4 days of incubation with OVA (100 μg/ml). *E*, IL-10 production by $CD4^+$ T cells after nonspecific stimulation. $CD4^+$ T cells were negatively selected and then stimulated in vitro with PMA (1 ng/ml) and ionomycin (0.1 μg/ml) for 2 days. IL-10 concentrations in the supernatants were measured. Data were obtained from four wells per group of mice. ##, $p < 0.01$; and ###, $p < 0.001$ (vs control mice).

treated with HGF demonstrated significantly reduced cell proliferation (Fig. 1*A*) and the production of IL-4 (Fig. 1*B*), IFN-γ (Fig. 1*C*), and IL-10 (Fig. 1*D*) upon stimulation with OVA-Ag. Then, we also confirmed that treatment with HGF in vivo significantly suppressed IL-10 production by $CD4^+$ T cells in response to nonspecific stimulation with PMA and ionomycin (Fig. 1*E*). These results indicated that HGF potently suppressed Ag-induced T cell priming with a down-regulation of IL-10 production.

HGF significantly suppresses T cell priming induced by CII/CFA

Then, we examined the immunosuppressive effect of HGF in the CIA model. DBA/1 mice were sensitized with CII/CFA and received a s.c. injection of gelatin or gelatin/rhHGF complex once on day 0. On day 10, spleen cells were obtained and then restimulated

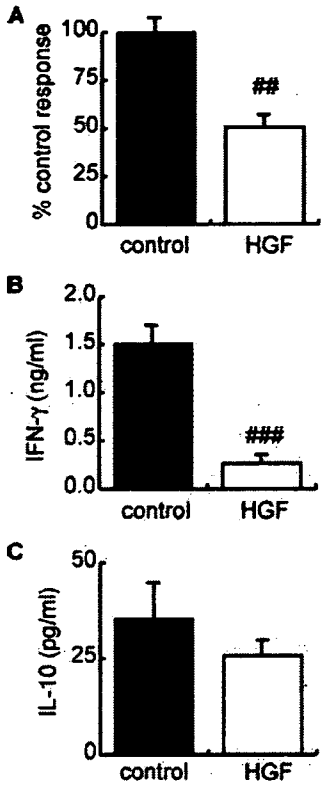

FIGURE 2. Controlled release of HGF in vivo potently suppresses T cell priming by CII/CFA. DBA/1 male mice were sensitized with CII/CFA and a few hours later, received a s.c. injection of gelatin (control) or gelatin/rhHGF (HGF) complex on day 0. On day 10, spleen cells were obtained from each group of mice and spleen cells (5×10^6 cells/ml) were restimulated with CII (10 μg/ml) in vitro. *A*, Cell proliferation after 3 days of incubation was measured by BrdU incorporation. Data are expressed as a percentage of the response compared with that of spleen cells from control mice. *B* and *C*, Production of IFN-γ after 3 days of incubation (*B*) and IL-10 after 4 days of incubation (*C*) was measured by ELISA. Data were obtained from four wells per group of mice. ##, $p < 0.01$ (vs control mice).

in vitro with CII. Spleen cells obtained from the mice treated with HGF demonstrated significantly reduced cell proliferation (Fig. 2*A*) and IFN-γ production (Fig. 2*B*). The production of IL-10 by spleen cells from mice treated with HGF also tended to decrease compared with that by cells from control mice (Fig. 2*C*). At this time point, IL-4 production was very low. We obtained almost the same results using femoral LN cells instead of spleen cells (data not shown). In preliminary experiments, we confirmed that the s.c. injection of HGF protein (10 μg/mouse/day) once daily on days 0–9 had no effect on CII/CFA-induced T cell priming (data not shown). These results indicated that the controlled release of HGF using the gelatin/rhHGF complex could suppress Ag-induced T cell priming independently of the kind of Ag and mouse strain and that this immunosuppressive effect might be exhibited without up-regulation of IL-10 production.

HGF significantly suppresses Ag-induced DC activation

We previously reported that HGF significantly suppressed DC functions such as Ag presentation and cytokine production, thus inhibiting OVA-induced not only Th2-type immune responses but also Th1-type immune responses (24). In the present study, we examined the mechanism of immunosuppression by HGF in CII/CFA-induced sensitization. DBA/1 mice were sensitized and treated as described above, and on day 10 DCs were purified from each group of mice. Then cytokine production by DCs after in vitro LPS stimulation was examined. Treatment with the HGF complex in vivo significantly suppressed the production of IL-10 (Fig. 3*A*), IL-12p70 (Fig. 3*B*), and IL-23 (Fig. 3*C*) by DCs after LPS stimulation. Moreover, compared with DCs from control mice, DCs from HGF-treated mice demonstrated a significantly decreased capacity to induce the proliferation of $CD4^+$ T cells (Fig. 3*D*) and the production of IL-10 (Fig. 3*E*) and IFN-γ (Fig. 3*F*) from $CD4^+$ T cells obtained from the CII/CFA-sensitized mice in the presence of CII in the medium. Moreover, we also confirmed that CD40 expression was reduced in DCs obtained from HGF-treated mice compared with that in DCs from control mice (Fig. 3*G*). These results suggested that HGF significantly suppressed DC function in the early stages of the Ag-induced immune response, thus suppressing Ag-induced $CD4^+$ T cell activation.

HGF up-regulates IL-10 production by immunocytes under continuous Ag stimulation

Next, we examined the effect of HGF on Ag-primed T cells using ex vivo and in vitro experiments. In ex vivo experiments, mice were sensitized with CII/CFA on day 0, received gelatin or gelatin/rhHGF complex on days 0 and 10, and spleen cells were collected on day 20 from each group of mice. Then the spleen cells were restimulated in vitro with CII. Spleen cells obtained from the mice treated with HGF demonstrated significantly increased IL-10 production (Fig. 4*A*). The production of IFN-γ by spleen cells from mice treated with HGF tended to decrease compared with that of cells from control mice (Fig. 4*B*). IL-4 production by spleen cells from each group of mice was very low and did not differ between each group at this time point (data not shown). We also confirmed that $CD4^+$ T cells obtained on day 20 from the mice treated with HGF demonstrated significantly increased IL-10 production after nonspecific PMA and ionomycin stimulation (Fig. 4*C*). Moreover, we examined the cytokine profile of splenic DCs purified on day 20 and found that IL-10 production by DCs from mice treated with HGF tended to increase compared with that of DCs from control mice (Fig. 4*D*), while IL-12p70 production by DCs was as significantly suppressed by HGF as it was on day 10 (Fig. 4*E*). These results indicated that, under continuous Ag-stimulation, HGF could induce IL-10-producing immunocytes including T cells and DCs. To confirm this possibility, we then conducted in vitro studies. Spleen cells obtained on day 10 from CII/CFA-sensitized mice were restimulated in vitro with CII in the presence or absence of HGF in the medium. Like the treatment with HGF in vivo, HGF in vitro significantly up-regulated IL-10 (Fig. 4*F*) production by splenocytes without affecting IFN-γ and IL-4 production (Fig. 4*G*).

HGF significantly reduces IL-17 production by T cells

We also examined the effect of HGF on the production of IL-17 by T cells. The femoral LN cells from HGF-treated mice produced significantly less IL-17 than those from control mice on days 10 (Fig. 5*A*) and 20 (Fig. 5*B*), although no significant difference was detected in spleens (data not shown).

Controlled release of HGF significantly suppresses development of CIA in mice

Then, we examined the effect of HGF on the development of experimental arthritis. DBA/1 mice were sensitized with CII/CFA on day 0 and received a booster injection of CII/IFA on day 21. Mice received s.c. injections of gelatin or gelatin/rhHGF complex on day 0 and every 10 days. The severity of the arthritis in the mice was scored on a scale of 0–4 for each limb. Progression of the

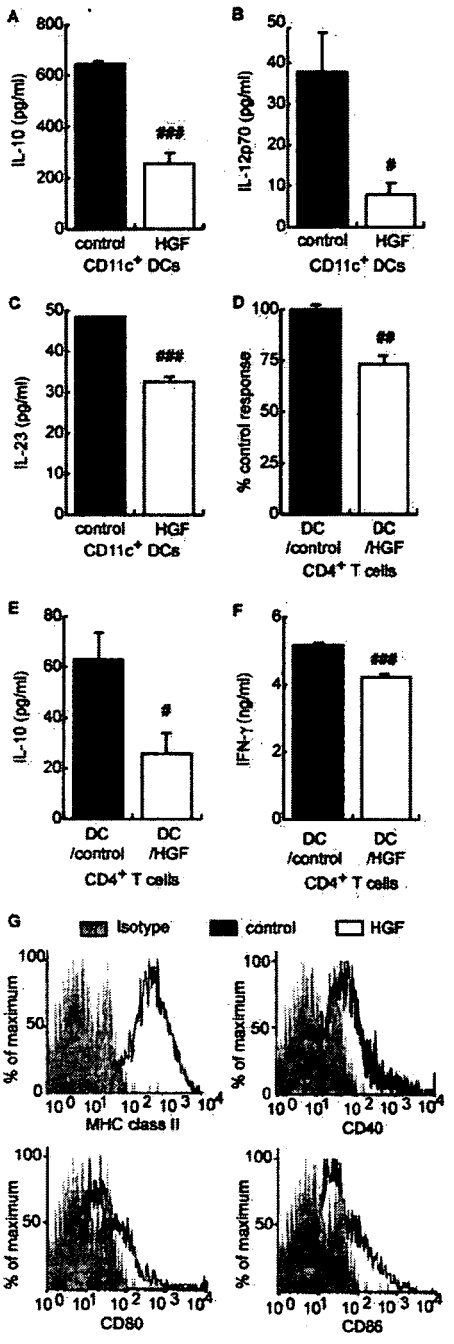

FIGURE 3. Controlled release of HGF in vivo potently suppresses DC functions, thus down-regulating Ag-induced $CD4^+$ T cell activation. Mice were treated as described in Fig. 2. On day 10, $CD11c^+$ DCs and $CD4^+$ T cells were purified from spleen cells as described in *Materials and Methods*. Then, the functions of DCs from each group of mice were examined. *A–C*, Cytokine production by DCs after LPS stimulation in vitro. DCs (1×10^6 cells/ml) from each group of mice were stimulated with LPS (1 μg/ml) in vitro. After 2 days, IL-10 (*A*), IL-12p70 (*B*), and IL-23 (*C*) in the supernatants were measured. *D–F*, Effects of DCs from each group of mice on the cell proliferation of and cytokine production by primed $CD4^+$ T cells. $CD4^+$ T cells (1×10^6 cells/ml) were obtained from control mice and cocultured with DCs (1×10^5 cells/ml) from each group of mice in the presence of CII (3 μg/ml for *D* and 10 μg/ml for *E* and *F*) in the medium. After 3 days (*D*), the cell proliferation of $CD4^+$ T cells was measured. After 4 days of incubation, the production by $CD4^+$ T cells of IL-10 (*E*) and IFN-γ (*F*) was measured. Data were obtained from three to four wells per group of mice. #, $p < 0.05$; ##, $p < 0.01$; ###, $p < 0.001$ (vs DCs from control mice). *G*, Effect of HGF on surface molecule expression on $CD11c^+$ DCs. The expression of MHC class II, CD40, CD80, and CD86 was examined by flow cytometry. Representative data from three independent experiments are shown.

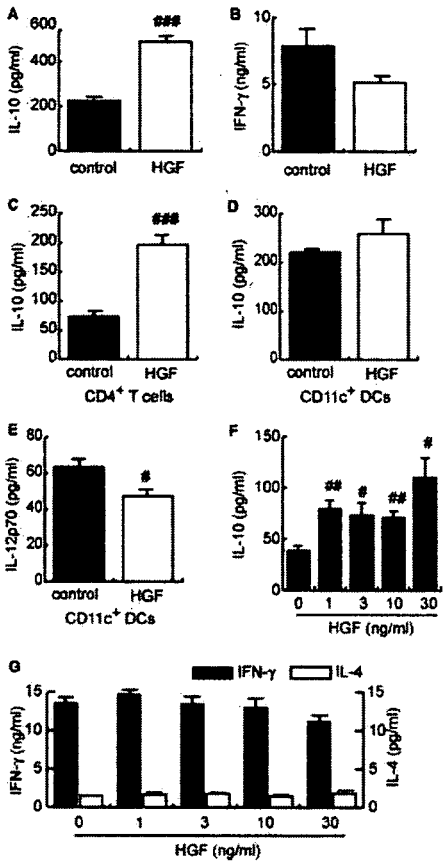

FIGURE 4. HGF significantly increased IL-10 production by Ag-primed immunocytes. *A–E*, Effect of treatment with HGF in vivo after Ag priming on cytokine production by spleen cells, $CD4^+$ T cells, or DCs. Mice were sensitized with CII/CFA on day 0. Mice also received gelatin (control) or gelatin/HGF complex (HGF) on days 0 and 10. On day 20, whole spleen cells, splenic $CD4^+$ T cells, or DCs were obtained from each group of mice. Then, spleen cells (5×10^6 cells/ml) were restimulated with CII (10 μg/ml) in vitro. Production of IL-10 (*A*) and IFN-γ (*B*) after 4 days of incubation was measured. $CD4^+$ T (1×10^6 cells/ml) cells were stimulated in vitro with PMA (1 ng/ml) and ionomycin (0.1 μg/ml) for 2 days, and IL-10 concentrations in the supernatants were measured (*C*). DCs (1×10^6 cells/ml) were stimulated with LPS (1 μg/ml) for 2 days, and IL-10 (*D*) and IL-12p70 (*E*) concentrations in the supernatants were measured. Data were obtained from four wells per group of mice. *F* and *G*, Effect of in vitro treatment with HGF on cytokine production by spleen cells induced by Ag restimulation. Mice were sensitized with CII/CFA on day 0, and spleen cells were obtained on day 10. Spleen cells (5×10^6 cells/ml) were restimulated with CII (10 μg/ml) in vitro in the presence or absence of rhHGF at several concentrations for 4 days. Concentrations of IL-10 (*F*), IFN-γ (■), and IL-4 (□) (*G*) in the supernatant were measured. #, $p < 0.05$; ##, $p < 0.01$; and ###, $p < 0.001$ (vs spleen cells, $CD4^+$ T cells, or DCs from control mice, respectively).

arthritis was evaluated until day 39 after immunization. On day 40, the most severely swollen hind paw was obtained from each mouse, and a histologic examination was conducted. HGF treatment significantly suppressed the severity (Fig. 6*A*) and incidence (Fig. 6*B*) of CII-induced arthritis. Histologic examination demonstrated that HGF potently reduced articular destruction such as cartilage destruction, synovial hypertrophy, pannus formation, and

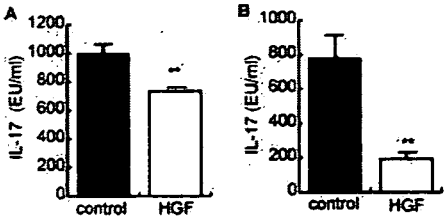

FIGURE 5. Treatment with gelatin/HGF complex in vivo potently suppresses IL-17 production. Mice were sensitized with CII/CFA and a few hours later received a s.c. injection of gelatin (control) or gelatin/rhHGF complex (HGF) on day 0. On day 10, femoral LN cells were obtained from each group of mice. Some mice also received additional treatment with gelatin (control) or gelatin/rhHGF complex on day 10 and femoral LN cells were obtained on day 20. Then the cells obtained on the indicated days were restimulated with CII (10 μg/ml) in vitro for 4 days and IL-17 concentrations in the supernatants were measured. IL-17 production by LN cells obtained from control mice on day 10 was defined as 1000 EU. *A*, IL-17 production by LN cells obtained on day 10. *B*, IL-17 production by LN cells obtained on day 20. ##, $p < 0.01$ (vs control mice).

bone erosion (Fig. 6, *C–F* and Table II). HGF significantly reduced CII-specific total IgG (Fig. 6*G*) and IgG2a (Fig. 6*H*) production. In a preliminary experiment, we confirmed that the s.c. injection of

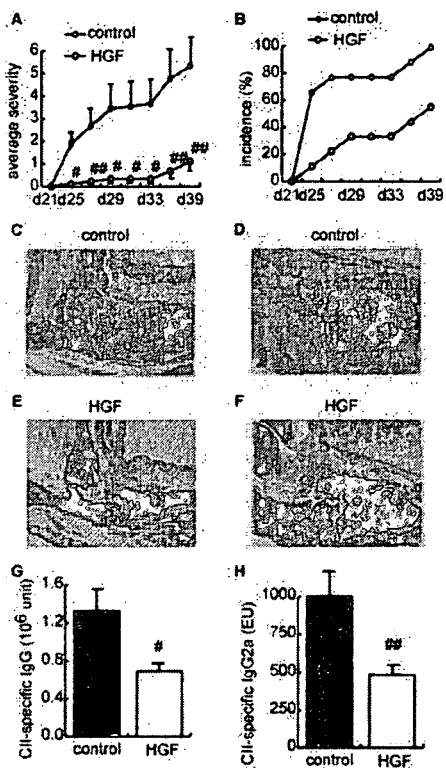

FIGURE 6. Treatment with gelatin/HGF complex in vivo significantly suppresses development of CIA. Arthritis was induced in DBA/1 mice by immunization with CII in Freund's complete adjuvant on day 0. On day 21, mice were injected s.c. with CII in Freund's incomplete adjuvant. Mice also received gelatin (control; $n = 9$) or gelatin/HGF complex (HGF; $n = 9$) on day 0 and every 10 days. *A*, Arthritis scores in the two groups. Clinical scores were determined as described in *Materials and Methods*. *B*, Incidence of arthritis in the two groups. *C–F*, H&E staining of representative hind paws from control mice (*C* and *D*) and mice treated with gelatin/HGF complex (*E* and *F*). Original magnification: ×16 for *C* and *D* and × 32 for *E* and *F*. *G* and *H*, CII-specific total IgG (*G*) and IgG2a (*H*) concentration in the sera obtained from each group of mice on day 40. Data were obtained from nine mice per group. #, $p < 0.05$; ##, $p < 0.01$ (vs control mice).

Table II. *Impact of treatment with HGF in the murine CIA model*[a]

Pathologic Category	Control	HGF
Cartilage	1.33 ± 0.441	0.111 ± 0.111[b]
Cellularity	1.22 ± 0.521	0.222 ± 0.222
Pannus	1.11 ± 0.455	0.111 ± 0.111
Bone erosion	1.11 ± 0.484	0.111 ± 0.111

[a] Data are the mean ± SEM pathologic score from nine animals per group (0, normal; 1, minimal; 2, mild; 3, moderate; and 4, marked).
[b] $p < 0.05$ vs control mice (Mann-Whitney *U* test).

HGF protein (10 μg/mouse/day) once daily on days 0–40 had no suppressive effect on the development of CII-induced arthritis (data not shown). These results indicated that controlled release of HGF could suppress Ag-induced arthritis.

Continuous treatment with HGF during Ag-induced chronic inflammation enhances Th2-type immune responses

Finally, we elucidated the mechanism of suppression by HGF in the chronic phase of arthritis. Mice were sensitized and then treated as described above. On day 40, spleen cells were obtained from each group of mice and restimulated in vitro with CII. Spleen cells obtained on day 40 from the mice treated with HGF demonstrated significantly reduced cell proliferation (Fig. 7*A*) and enhanced IL-10 production (Fig. 7*B*) in response to in vitro CII restimulation. Interestingly, in this chronic phase of Ag-induced

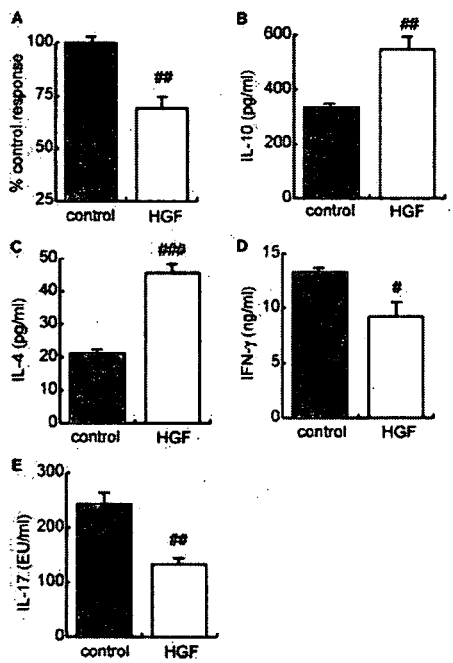

FIGURE 7. In vivo treatment with gelatin/HGF complex (HGF) in the presence of persistent Ag stimulation enhances Ag-specific Th2-type immune responses. Mice were treated as described in Fig. 6. On day 40, spleen cells were collected from each group of mice. *A–E*, Spleen cell responses to in vitro CII (10 μg/ml) stimulation were examined. *A*, Cell proliferation after 3 days of incubation. Data are expressed as a percentage of the response compared with that of spleen cells from control mice. *B–E*, Concentrations of IL-10 (*B*) and IL-4 (*C*) after 5 days of incubation, IFN-γ after 4 days of incubation (*D*), and IL-17 (*E*) after 3 days of incubation in the supernatants were measured. Data were obtained from four wells per group of mice. #, $p < 0.05$; ##, $p < 0.01$; and ###, $p < 0.001$ (vs spleen cells from control mice).

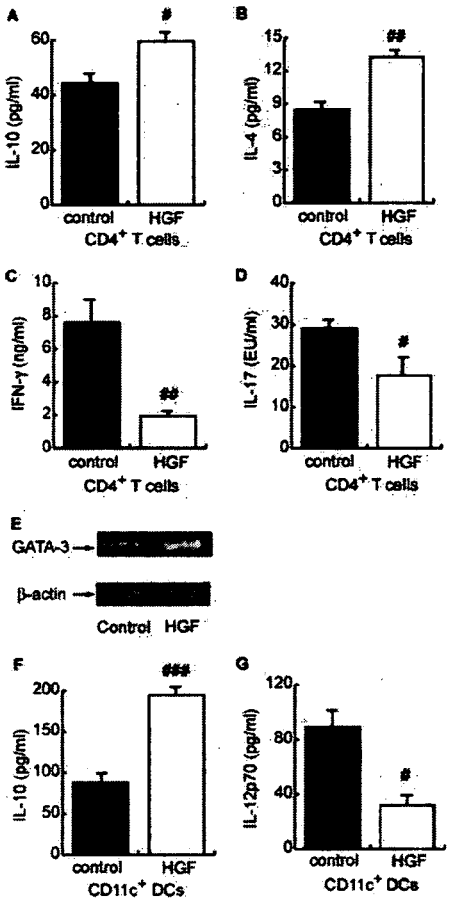

FIGURE 8. Effect of repeated treatment with gelatin/HGF complex (HGF) in vivo on cytokine production by $CD4^+$ T cells and DCs. Mice were treated as described in Fig. 6. On day 40, splenic $CD4^+$ T cells and DCs were purified from each group of mice. Then, $CD4^+$ T cells (1×10^6 cells/ml) were stimulated with PMA (1 ng/ml) and ionomycin (0.1 μg/ml) and IL-10 production after 1 day of incubation (*A*), IL-4 production after 20 h of incubation (*B*), and IFN-γ (*C*) and IL-17 (*D*) production after 2 days of incubation were measured. *E*, GATA-3 mRNA expression in $CD4^+$ T cells. RNA was extracted from splenic $CD4^+$ T cells and then RT-PCRs for GATA-3 and β-actin were conducted. *F* and *G*, DCs were stimulated with LPS (1 μg/ml) for 2 days, and IL-10 (*F*) and IL-12p70 (*G*) concentrations in the supernatants were measured. Data were obtained from three to four wells per group of mice. #, $p < 0.05$; ##, $p < 0.01$; and ###, $p < 0.001$ (vs $CD4^+$ T cells or DCs from control mice, respectively).

immune response, spleen cells obtained from control mice produced a significant amount of IL-4 in response to Ag restimulation, and spleen cells from HGF-treated mice demonstrated significantly enhanced production of IL-4 after Ag restimulation (Fig. 7*C*) with down-regulation of cytokine production for IFN-γ (Fig. 7*D*) and IL-17 (Fig. 7*E*). Further, the cytokine profiles of $CD4^+$ T cells from each group of mice after PMA and ionomycin stimulation (Fig. 8, *A–D*) were the same as those of spleen cells after CII restimulation (Fig. 7, *B–E*). We also confirmed that treatment with HGF enhanced mRNA expression of the transcription factor GATA-3, which is known as a master gene for Th2 cell development (45), in splenic $CD4^+$ T cells obtained on day 40 (Fig. 8*E*). Moreover, we found that continuous treatment with HGF in vivo significantly increased IL-10 production (Fig. 8*F*) and decreased IL-12p70 production (Fig. 8*G*) by DCs after LPS stimulation. These results indicated that repeated treatment with HGF in chronic inflammation could induce Th2-type immune responses with up-regulation of IL-10 production by DCs.

Discussion

The results of the present study clearly demonstrated that HGF strongly suppresses collagen-induced immune responses, thus attenuating experimental arthritis. In the early phase, systemic delivery of HGF suppressed the activation of DCs in the spleen that was provoked by sensitization with CII, thus down-regulating CII-induced $CD4^+$ T cell activation. During continuous Ag stimulation, HGF up-regulated IL-10 production by immunocytes. Further, the delivery of HGF attenuated the severity and incidence of arthritis in the CIA model with down-regulation of IL-17 production. To our knowledge, this is the first report that clearly demonstrates the effect of HGF on immune-mediated arthritis.

The presentation of Ag by APCs to T cells initiates the differentiation of naive Th cells into the effector T cells. During the differentiation into each phenotype such as Th1, Th2, or regulatory T (Treg) cells, the expression of costimulatory molecules on APCs and the cytokine profile produced by APCs play a critical role (46). Among various APCs, DCs are most efficient and crucial (47).

Recent articles reported the effect of HGF on DC functions (24, 48). Rutella et al. (48) reported that, in in vitro experiments, HGF suppresses alloantigen-presenting capacity, modulates the costimulatory molecule expression and cytokine production of DCs, and generates DCs that induce Treg cells ("tolerogenic DCs"). In contrast, we reported that HGF potently suppresses Ag-presenting capacity and IL-12p70 production of DCs, thus inhibiting the development of both Th1- and Th2-type immune responses induced by OVA (24).

In the present study, we confirmed that treatment with HGF in vivo suppressed the production of both IL-10 and IL-12p70 by CII/CFA-induced DCs (Fig. 3, *A* and *B*). When the DCs and $CD4^+$ T cells were cocultured in the presence of CII, DCs from HGF-treated mice showed a reduced capacity to present Ag to $CD4^+$ T cells (Fig. 3*D*) and to induce IFN-γ and IL-10 production by CII/CFA-primed $CD4^+$ T cells compared with DCs obtained from CII/CFA-sensitized control mice (Fig. 3, *E* and *F*). Moreover, we also found that HGF decreased CD40 expression on DCs (Fig. 3*G*), which was consistent with our previous study (24). We also confirmed that HGF potently inhibited CII/CFA-induced T cell priming (Fig. 2). Based on these results, in a situation such as Ag-induced T cell priming in which DCs play an essential role, HGF would suppress immune responses through down-regulation of DC function.

Then, with continuous Ag stimulation, HGF up-regulated IL-10 production by immunocytes including T cells (Fig. 4, *A*, *C*, and *F*). IL-10 is an immunosuppressive and regulatory cytokine (49–51). This is consistent with a recent report that HGF reduced acute and chronic rejection of allografts with the increased expression of IL-10 in a mouse model of allogenic heart transplantation (22). The exact mechanism of induction of IL-10-producing T cells remains unclear. Generally, exogenous IL-10 itself plays an important role in the induction of IL-10-producing T cells (50, 51). In our study, HGF did not directly increase IL-10 production when added to cocultures of DCs and $CD4^+$ T cells obtained from CII/CFA-sensitized control mice on day 10 in the presence of CII (data not shown). HGF did not increase PMA and ionomycin-induced production of IL-10 by $CD4^+$ T cells obtained from CII/CFA-sensitized mice (data not shown). Moreover, to clarify whether IL-10 was produced by $Foxp3^+$ Treg cells, we also examined the percentage and the absolute number of $CD4^+$ ($CD25^+$) $Foxp3^+$ cells in the spleens or draining LNs of each group of mice on days 10, 20, and 40. We found that treatment with HGF in vivo did not

increase $CD4^+Foxp3^+$ Treg cells in spleens and LNs in the present study (data not shown). Treatment of splenocytes with HGF in vitro during CII restimulation did not increase $Foxp3^+$ Treg cells either. In contrast, repeated treatment with HGF in vivo gradually increased IL-10 production by DCs (Figs. 4*D* and 8*F*). These results indicated that the augmented IL-10 production by $CD4^+$ T cells was not mediated by $Foxp3^+$ Treg cells but, at least in vivo. by up-regulation of IL-10 production by DCs after repeated HGF treatment. The precise mechanism of induction of IL-10-producing $CD4^+$ T cells by HGF is not clear at present and should be further investigated.

IL-10 also enhances the formation of Th2 cells by down-regulating IL-12 production by DCs (52). Moreover, some reports also emphasize the importance of IL-10 in the induction of Th2 cells (53, 54). As described above, after T cells were primed with Ag, HGF in the presence of continuous Ag stimulation increased IL-10 production by immunocytes, including DCs, along with suppression of IL-12 production by DCs (Figs. 4, 7, and 8), indicating that under continuous Ag stimulation HGF could induce Th2-type immune responses in the chronic phase. In fact, in the chronic phase of CII-induced immune responses, repeated treatment with HGF up-regulated both IL-4 and IL-10 production in T cells (Figs. 7 and 8). These results were consistent with a recent report that HGF ameliorates the progression of experimental autoimmune myocarditis with the induction of Th2 cytokines (23). We also confirmed that HGF enhanced mRNA expression of GATA-3, which specifies Th2 cell development, in $CD4^+$ T cells in the chronic inflammatory phase (Fig. 8*E*). Th2-type immune responses suppress Th1-type immune responses (55), and a recent study reported that IL-4 significantly suppresses the development of Th17 cells, a new subset of effector $CD4^+$ T cells distinct from Th1 or Th2 cells (56). However, in the current study we found that neutralization of IL-4 in vitro did not increase IL-17 production by splenocytes after CII restimulation (data not shown). Collectively, HGF would enhance Th2-type immune responses in chronic inflammation, thus inhibiting both Th1- and Th17-type responses at least in vivo.

Recent studies clarified that IL-17 produced by Th17 cells has a crucial role in the induction of autoimmune tissue injury (30–32, 57, 58). Accumulating evidence indicates that IL-17 plays an essential role not only in the induction of autoimmune arthritis (30, 31) but also in the subsequent bone destruction (32). In the current study, HGF potently suppressed IL-17 production by draining LN cells after in vitro CII restimulation in the early stage of Ag-induced immune responses (Fig. 5). Further, in addition to the sensitization phase, even in the chronic inflammation phase with joint destruction HGF significantly suppressed IL-17 production by spleen cells (Fig. 7*E*). Moreover, HGF significantly suppressed DC production of IL-23 (Fig. 3*C*), which is now recognized as a very important cytokine for IL-17 secretion from activated $CD4^+$ T cells (57, 59). These results indicated that HGF would be beneficial in treating autoimmune arthritis.

TGF-β is an immunosuppressive growth factor. Some phenotypes of T cells function as Treg cells by producing TGF-β. In contrast, the role of TGF-β in the induction of the Th17 cell lineage to promote an autoimmune response has been recently highlighted (52, 60, 61). Generally, HGF counteracts the biological functions of TGF-β such as promoting fibrosis (13, 14). In the immune response, however, the relation between HGF and TGF-β differs among experimental systems. HGF suppresses acute and chronic rejection in a mouse model of cardiac allograft transplantation with unexpectedly enhanced expression of TGF-β mRNA (22). In contrast, in allergic airway inflammation HGF did not up-regulate TGF-β production in the lung (24). In the present study on arthritis, HGF reduced mRNA expression of TGF-β in $CD4^+$ T cells at both early and chronic phases (data not shown).

Generally, exogenously administered HGF proteins vanish from organs within several hours (44). In a preliminary study, we confirmed that s.c. injection of HGF protein (10 μg per mouse) once daily failed to suppress the Ag-induced T cell priming and development of CII-induced arthritis (data not shown). Previously, we used a hydrodynamic-based transfer system to deliver HGF effectively and confirmed that a slight but continuous up-regulation of HGF protein in the sera potently suppressed OVA/alum-induced T cell priming and allergic airway inflammation (24). However, this delivery system could not be applied to an experimental model of arthritis due to an anatomical narrowing of the tail vein provoked by injection of CII/CFA into the subcutis of the tail. Thus, to achieve a controlled release of HGF, we adopted biodegradable gelatin hydrogels as carriers of HGF. We previously confirmed that when this gelatin/HGF complex was s.c. injected into mice, HGF was delivered under a controlled release based on hydrogel degradation and that the degradation occurred over 10 days (37). We reconfirmed that controlled release of HGF was achieved using a gelatin/rhHGF complex by examining the time course of concentration of HGF in the sera (Table I). In this study, the controlled release of HGF potently suppressed Ag-induced T cell priming and development of CII-induced arthritis. Thus, gelatin hydrogels would be an ideal carrier for HGF to exhibit its biological effects, and further application in various models can be expected.

Pulmonary fibrosis is often associated with RA and is one of the major causes of death in RA patients (62). To date, several articles, including our own, reported that HGF inhibits the progression of experimental pulmonary fibrosis (15, 63, 64). Considering the simultaneous effect on pulmonary fibrosis and arthritis, HGF could be an attractive tool in treating RA with pulmonary involvement in a clinical situation. In contrast, in the clinical use of HGF the possibility of promoting tumor progression should be considered. Therefore, for practical usage of HGF in clinical situations further studies should be performed.

In summary, our results in the present study indicated that HGF could exhibit its immunosuppressive effects in different manners at different stages of immune response. In the early phase of Ag-induced immune responses HGF potently suppressed DC function, thus inhibiting T cell priming by Ag. In contrast, during chronic inflammation HGF gradually increased IL-10 production by DCs, which subsequently induced IL-10 producing T cells and Th2-type immune responses. The precise mechanism should be further investigated in detail.

Acknowledgment

We thank K. Kurosaki for technical assistance.

Disclosures

The authors have no financial conflict of interest.

References

1. Gohda, E., H. Tsubouchi, H. Nakayama, S. Hirono, O. Sakiyama, K. Takahashi, H. Miyazaki, S. Hashimoto, and Y. Daikuhara. 1988. Purification and partial characterization of hepatocyte growth factor from plasma of a patient with fulminant hepatic failure. *J. Clin. Invest.* 81: 414–419.
2. Miyazawa, K., H. Tsubouchi, D. Naka, K. Takahashi, M. Okigaki, N. Arakaki, H. Nakayama, S. Hirono, O. Sakiyama, K. Takahashi, et al. 1989. Molecular cloning and sequence analysis of cDNA for human hepatocyte growth factor. *Biochem. Biophys. Res. Commun.* 163: 967–973.
3. Nakamura, T., T. Nishizawa, M. Hagiya, T. Seki, M. Shimonishi, A. Sugimura, K. Tashiro, and S. Shimizu. 1989. Molecular cloning and expression of human hepatocyte growth factor. *Nature* 342: 440–443.
4. Stoker, M., E. Gherardi, M. Perryman, and J. Gray. 1987. Scatter factor is a fibroblast-derived modulator of epithelial cell mobility. *Nature* 327: 239–242.

5. Zarnegar, R., and G. K. Michalopoulos. 1995. The many faces of hepatocyte growth factor: from hepatopoiesis to hematopoiesis. *J. Cell Biol.* 129: 1177–1180.
6. Bardelli, A., P. Longati, D. Albero, S. Goruppi, C. Schneider, C. Ponzetto, and P. M. Comoglio. 1996. HGF receptor associates with the anti-apoptotic protein BAG-1 and prevents cell death. *EMBO J.* 15: 6205–6212.
7. Huh, C. G., V. M. Factor, A. Sanchez, K. Uchida, E. A. Conner, and S. S. Thorgeirsson. 2004. Hepatocyte growth factor/*c-met* signaling pathway is required for efficient liver regeneration and repair. *Proc. Natl. Acad. Sci. USA* 101: 4477–4482.
8. Trusolino, L., and P. M. Comoglio. 2002. Scatter-factor and semaphoring receptors: cell signaling for invasive growth. *Nat. Rev. Cancer* 2: 289–300.
9. Imaizumi, Y., H. Murota, S. Kanda, Y. Hishikawa, T. Koji, T. Taguchi, Y. Tanaka, Y. Yamada, S. Ikeda, T. Kohno, et al. 2003. Expression of the c-met proto-oncogene and its possible involvement in liver invasion in adult T-cell leukemia. *Clin. Cancer Res.* 9: 181–187.
10. Siegfried, J. M., L. A. Weissfeld, P. Singh-Kaw, R. J. Weyant, J. R. Testa, and R. J. Landreneau. 1997. Association of immunoreactive hepatocyte growth factor with poor survival in resectable non-small cell lung cancer. *Cancer Res.* 57: 433–439.
11. To, Y., M. Dohi, K. Matsumoto, R. Tanaka, A. Sato, K. Nakagome, T. Nakamura, and K. Yamamoto. 2002. A two-way interaction between hepatocyte growth factor and interleukin-6 in tissue invasion of lung cancer cell line. *Am. J. Respir. Cell Mol. Biol.* 27: 220–226.
12. Wislez, M., N. Rabbe, J. Marchal, B. Milleron, B. Crestani, C. Mayaud, M. Antoine, P. Soler, and J. Cadranel. 2003. Hepatocyte growth factor production by neutrophils infiltrating bronchoalveolar subtype pulmonary adenocarcinoma: role in tumor progression and death. *Cancer Res.* 63: 1405–1412.
13. Mizuno, S., T. Kurosawa, K. Matsumoto, Y. Mizuno-Horikawa, M. Okamoto, and T. Nakamura. 1998. Hepatocyte growth factor prevents renal fibrosis and dysfunction in a mouse model of chronic renal disease. *J. Clin. Invest.* 101: 1827–1834.
14. Ueki, T., Y. Kaneda, H. Tsutsui, K. Nakanishi, Y. Sawa, R. Morishita, K. Matsumoto, T. Nakamura, H. Takahashi, E. Okamoto, and J. Fujimoto. 1999. Hepatocyte growth factor gene therapy of liver cirrhosis in rats. *Nat. Med.* 5: 226–230.
15. Dohi, M., T. Hasegawa, K. Yamamoto, and B. C. Marshall. 2000. Hepatocyte growth factor attenuates collagen accumulation in a murine model of pulmonary fibrosis. *Am. J. Respir. Crit. Care Med.* 162: 2302–2307.
16. van der Voort, R., T. E. I. Taher, R. M. J. Keehnen, L. Smit, M. Groenink, and S. T. Pals. 1997. Paracrine regulation of germinal center B cell adhesion through the c-met-hepatocyte growth factor/scatter factor pathway. *J. Exp. Med.* 185: 2121–2131.
17. Weimar, I. S., D. de Jong, E. J. Muller, T. Nakamura, J. M. van Gorp, G. C. de Gast, and W. R. Gerritsen. 1997. Hepatocyte growth factor/scatter factor promotes adhesion of lymphoma cells to extracellular matrix molecules via $\alpha_4\beta_1$ and $\alpha_5\beta_1$ integrins. *Blood* 89: 990–1000.
18. Adams, D. H., L. Harvath, D. P. Bottaro, R. Interrante, G. Catalano, Y. Tanaka, A. Strain, S. G. Hubscher, and S. Shaw. 1994. Hepatocyte growth factor and macrophage inflammatory protein 1b: structurally distinct cytokines that induce rapid cytoskeletal changes and subset-preferential migration in T cells. *Proc. Natl. Acad. Sci. USA* 91: 7144–7148.
19. Kurz, S. M., S. S. Diebold, T. Hieronymus, T. C. Gust, P. Bartunek, M. Sachs, W. Birchmeier, and M. Zenke. 2002. The impact of c-met/scatter factor receptor on dendritic cell migration. *Eur. J. Immunol.* 32: 1832–1838.
20. Scarpino, S., A. Stoppacciaro, F. Ballerini, M. Marchesi, M. Prat, M. C. Stella, S. Sozzani, P. Allavena, A. Mantovani, and L. P. Ruco. 2000. Papillary carcinoma of the thyroid: hepatocyte growth factor (HGF) stimulates tumor cells to release chemokines active in recruiting dendritic cells. *Am. J. Pathol.* 156: 831–837.
21. Kretzschmar, M., J. Doody, and J. Massague. 1997. Opposing BMP and EGF signaling pathways converge on the TGF-β family mediator Smad1. *Nature* 389: 618–622.
22. Yamamura, K., K. Ito, K. Tsukioka, Y. Wada, A. Makiuchi, M. Sakaguchi, T. Akashima, M. Fujimori, Y. Sawa, R. Morishita, et al. 2004. Suppression of acute and chronic rejection by hepatocyte growth factor in a murine model of cardiac transplantation. *Circulation* 110: 1650–1657.
23. Futamatsu, H., J. Suzuki, S. Mizuno, N. Koga, S. Adachi, H. Kosuge, Y. Maejima, K. Hirao, T. Nakamura, and M. Isobe. 2005. Hepatocyte growth factor ameliorates the progression of experimental autoimmune myocarditis: a potential role for induction of T helper 2 cytokines. *Circ. Res.* 96: 823–830.
24. Okunishi, K., M. Dohi, K. Nakagome, R. Tanaka, S. Mizuno, K. Matsumoto, J. Miyazaki, T. Nakamura, and K. Yamamoto. 2005. A novel role of hepatocyte growth factor as an immune regulator through suppressing dendritic cell function. *J. Immunol.* 175: 4745–4753.
25. Ito, W., A. Kanehiro, K. Matsumoto, A. Hirano, K. Ono, H. Maruyama, M. Kataoka, T. Nakamura, E. W. Gelfand, and M. Tanimoto. 2005. Hepatocyte growth factor attenuates airway hyperresponsiveness, inflammation, and remodeling. *Am. J. Respir. Cell Mol. Biol.* 32: 268–280.
26. Kuroiwa, T., T. Iwasaki, T. Imado, M. Sekiguchi, J. Fujimoto, and H. Sano. 2006. Hepatocyte growth factor prevents lupus nephritis in a murine model of chronic graft-versus-host disease. *Arthritis. Res. Ther.* 8: R123.
27. Hale, L. P., and B. F. Haynes. 2001. Pathology of rheumatoid arthritis and associated disorders. In *Arthritis and Allied Conditions: A Textbook of Rheumatology*, 14th Ed., Vol. 1. W. J. Koopman, ed. Williams & Wilkins Press, Baltimore, pp. 1103–1127.
28. Dolhain, R. J., A. N. van der Heiden, N. T. ter Haar, F. C. Breedveld, and A. M. Miltenburg. 1996. Shift toward T lymphocytes with a T helper 1 cytokine-secretion profile in the joints of patients with rheumatoid arthritis. *Arthritis Rheum.* 39: 1961–1969.
29. Smolen, J. S., M. Tohidast-Arkad, A. Gal, M. Kunaver, G. Eberl, P. Zenz, A. Falus, and G. Steiner. 1996. The role of T-lymphocytes and cytokines in rheumatoid arthritis. *Scand. J. Rheumatol.* 25: 1–4.
30. Miossec, P. 2003. Interleukin-17 in rheumatoid arthritis. *Arthritis Rheum.* 46: 594–601.
31. Nakae, S., S. Saijo, R. Horai, K. Sudo, S. Mori, and Y. Iwakura. 2003. IL-17 production from activated T cells is required for the spontaneous development of destructive arthritis in mice deficient in IL-1 receptor antagonist. *Proc. Natl. Acad. Sci. USA* 100: 5986–5990.
32. Sato, K., A. Suematsu, K. Okamoto, A. Yamaguchi, Y. Morishita, Y. Kadono, S. Tanaka, T. Kodama, S. Akira, Y. Iwakura, et al. 2006. Th17 functions as an osteoclastgenic helper T cell subset that links T cell activation and bone destruction. *J. Exp. Med.* 203: 2673–2682.
33. Maruotti, N., F. P. Cantatore, E. Crivellato, A. Vacca, and D. Ribatti. 2006. Angiogenesis in rheumatoid arthritis. *Histol. Histopathol.* 21: 557–566.
34. Koch, A. E., M. M. Halloran, S. Hosaka, M. R. Shah, C. J. Haskell, S. K. Baker, R. J. Panos, G. K. Haines, G. L. Bennett, R. M. Pope, and N. Ferrara. 1996. Hepatocyte growth factor. A cytokine mediating endothelial migration in inflammatory arthritis. *Arthritis Rheum.* 39: 1566–1575.
35. Yukioka, K., M. Inaba, Y. Furumitsu, M. Yukioka, T. Nishino, H. Goto, Y. Nishizawa, and H. Morii. 1994. Levels of hepatocyte growth factor in synovial fluid and serum of patients with rheumatoid arthritis and release of hepatocyte growth factor by rheumatoid synovial fluid cells. *J. Rheumatol.* 21: 2184–2189.
36. Feuerherm, A. J., M. Borset, C. Seidel, A. Sundan, L. Leistad, M. Ostensen, and A. Faxvaag. 2001. Elevated levels of osteoprotegerin (OPG) and hepatocyte growth factor (HGF) in rheumatoid arthritis. *Scand. J. Rheumatol.* 30: 229–234.
37. Ozeki, M., T. Ishii, Y. Hirano, and Y. Tabata. 2001. Controlled release of hepatocyte growth factor from gelatin hydrogels based on hydrogel degradation. *J. Drug. Target.* 9: 461–471.
38. Oe, S., Y. Fukunaka, T. Hirose, Y. Yamaoka, and Y. Tabata. 2003. A trial on regeneration therapy of rat liver cirrhosis by controlled release of hepatocyte growth factor. *J. Control. Release* 88: 193–200.
39. Okunishi, K., M. Dohi, K. Nakagome, R. Tanaka, and K. Yamamoto. 2004. A novel role of cysteinyl leukotrienes to promote dendritic cell activation in the antigen-induced immune responses in the lung. *J. Immunol.* 173: 6393–6402.
40. Kuroda, E., and U. Yamashita. 2003. Mechanisms of enhanced macrophage-mediated prostaglandin E_2 production and its suppressive role in Th1 activation in Th2-dominant BALB/c mice. *J. Immunol.* 170: 757–764.
41. Dabbagh, K., M. E. Dahl, P. Stepick-Biek, and D. B. Lewis. 2002. Toll-like receptor 4 is required for optimal development of Th2 immune responses: role of dendritic cells. *J. Immunol.* 168: 4524–4530.
42. Sagawa, K., K. Nagatani, Y. Komagata, and K. Yamamoto. 2005. Angiotensin receptor blockers suppress antigen-specific T cell responses and ameliorate collagen-induced arthritis in mice. *Arthritis Rheum.* 52: 1920–1928.
43. Nakagome, K., M. Dohi, K. Okunishi, Y. Komagata, K. Nagatani, R. Tanaka, J. Miyazaki, and K. Yamamoto. 2005. In vivo IL-10 gene delivery suppresses airway eosinophilia and hyperreactivity by down-regulating APC functions and migration without impairing the antigen-specific systemic immune response in a mouse model of allergic airway inflammation. *J. Immunol.* 174: 6955–6966.
44. Michalopoulos, G. K., and R. Appasamy. 1993. Metabolis of HGF-SF and its role in liver regeneration. *EXS* 65: 275–283.
45. Zheng, W., and R. A. Flavell. 1997. The transcription factor GATA-3 is necessary and sufficient for Th2 cytokine gene expression in CD4 T cells. *Cell* 89: 587–596.
46. Kapsenberg, M. L. 2003. Dendritic-cell control of pathogen-driven T-cell polarization. *Nat. Rev. Immunol.* 3: 984–993.
47. Banchereau, J., and R. M. Steinman. 1998. Dendritic cells and the control of immunity. *Nature* 392: 245–252.
48. Rutella, S., G. Bonanno, A. Procoli, A. Mariotti, D. G. de Ritis, A. Curti, S. Danese, G. Pessina, S. Pandolfi, F. Natoni, et al. 2006. Hepatocyte growth factor favors monocyte differentiation into regulatory interleukin (IL)-$10^{+/+}$IL-$12^{low/neg}$ accessory cells with dendritic-cell features. *Blood* 108: 218–227.
49. Fehérvari, Z., and S. Sakaguchi. 2004. $CD4^+$ Tregs and immune control. *J. Clin. Invest.* 114: 1209–1217.
50. Groux, H., A. O'Garra, M. Bigler, M. Rouleau, S. Antonenko, J. E. de Vries, and M. G. Roncarolo. 1997. A $CD4^+$ T-cell subset inhibits antigen-specific T-cell responses and prevents colitis. *Nature* 389: 737–742.
51. Hawrylowicz, C. M., and A. O'Garra. 2005. Potential role of interleukin-10-secreting regulatory T cells in allergy and asthma. *Nat. Rev. Immunol.* 5: 271–283.
52. De Smedt, T., M. Van Mechelen, G. De Becker, J. Urbain, O. Leo, and M. Moser. 1997. Effect of interleukin-10 on dendritic cell maturation and function. *Eur. J. Immunol.* 27: 1229–1235.
53. Liu, L., B. E. Rich, J. Inobe, W. Chen, and H. L. Weiner. 1998. Induction of Th2 cell differentiation in the primary immune response: dendritic cells isolated from adherent cell culture treated with IL-10 prime naive $CD4^+$ T cells to secret IL-4. *Int. Immunol.* 10: 1017–1026.
54. Ballic, A., Y. M. Harcus, M. D. Taylor, F. Brombacher, and R. M. Maizels. 2006. IL-4R signaling is required to induce IL-10 for the establishment of Th2 dominance. *Int. Immunol.* 18: 1421–1431.

55. Boehm, U., T. Klamp, M. Groot, and J. C. Howard. 1997. Cellular responses to interferon-γ. *Annu. Rev. Immunol.* 15: 749–795.
56. Mangan, P. R., L. E. Harrington, D. B. O'Quinn, W. S. Helms, D. C. Bullard, C. O. Elson, R. D. Hatton, S. M. Wahl, T. R. Schoeb, and C. T. Weaver. 2006. Transforming growth factor-β induces development of the Th17 lineage. *Nature* 441: 231–234.
57. Langrish, C. L., Y. Chen, W. M. Blumenschein, J. Mattson, B. Basham, S. D. Sedgwick, T. McClanahan, R. A. Kastelein, and D. J. Cua. 2005. IL-23 drives a pathogenic T cell population that induces autoimmune inflammation. *J. Exp. Med.* 201: 233–240.
58. Park, H., Z. Li, X. O. Yang, S. H. Chang, R. Nurieva, Y. H. Wang, Y. Wang, L. Hood, Z. Zhu, Q. Tian, and C. Dong. 2005. A distinct lineage of $CD4^+$ T cells regulates tissue inflammation by producing interleukin 17. *Nat. Immunol.* 6: 1133–1141.
59. Aggarwal, S., N. Ghilardi, M. H. Xie, F. J. de Sauvage, and A. L. Gurney. 2003. Interleukin-23 promotes a distinct CD4 T cell activation state characterized by the production of interleukin-17. *J. Biol. Chem.* 278: 1910–1914.
60. Veldhoen, M., R. J. Hocking, C. J. Atkins, R. M. Locksley, and B. Stockinger. 2006. TGFβ in the context of an inflammatory cytokine milieu supports de novo differentiation of IL-17-producing T cells. *Immunity* 24: 179–189.
61. Bettelli, E., Y. Carrier, W. Gao, T. Korn, T. B. Strom, M. Oukka, H. L. Weiner, and V. K. Kuchroo. 2006. Reciprocal developmental pathways for the generation of pathogenic effector Th17 and regulatory T cell. *Nature* 441: 235–238.
62. Jindal, S. K., and R. Agarwal. 2005. Autoimmunity and interstitial lung disease. *Curr. Opin. Pulm. Med.* 11: 438–446.
63. Yaekashiwa, M., S. Nakayama, K. Ohnuma, T. Sakai, T. Abe, K. Satoh, K. Matsumoto, T. Nakamura, T. Takahashi, and T. Nukiwa. 1997. Simultaneous or delayed administration of hepatocyte growth factor equally represses the fibrotic changes in murine lung injury induced by bleomycin. *Am. J. Respir. Crit. Care Med.* 156: 1937–1944.
64. Watanabe, M., M. Ebina, F. M. Orson, A. Nakamura, K. Kubo, K. Kubota, D. Koinuma, K. Akiyama, M. Maemondo, S. Okouchi, et al. 2005. Hepatocyte growth factor gene transfer to alveolar septa for effective suppression of lung fibrosis. *Mol. Ther.* 12: 58–67.

Available online at www.sciencedirect.com
SCIENCE DIRECT
ELSEVIER
Biochemical and Biophysical Research Communications 341 (2006) 94–100
BBRC
www.elsevier.com/locate/ybbrc

Identification of citrullinated eukaryotic translation initiation factor 4G1 as novel autoantigen in rheumatoid arthritis

Yuko Okazaki [a], Akari Suzuki [b], Tetsuji Sawada [a], Miyako Ohtake-Yamanaka [b], Tetsufumi Inoue [c], Terumitsu Hasebe [d], Ryo Yamada [b], Kazuhiko Yamamoto [a,b,*]

[a] *Department of Allergy and Rheumatology, Graduate School of Medicine, The University of Tokyo, Tokyo, Japan*
[b] *Laboratory for Rheumatic Diseases, SNP Research Center, The Institute of Physical and Chemical Research (RIKEN), Kanagawa, Japan*
[c] *Health Administration Center, Tokyo University of Foreign Studies, Tokyo, Japan*
[d] *Center for Materials Science, Department of Mechanical Engineering, Keio University School of Science and Technology, Kanagawa, Japan*

Received 12 December 2005
Available online 6 January 2006

Abstract

Antibodies against citrullinated proteins are highly specific for rheumatoid arthritis. We previously reported that functional variants of the gene encoding peptidylarginine deiminase type 4 were closely associated with RA. The purpose of this study was to investigate the citrullinated autoantigens recognized by serum samples from patients with RA. The human chondrocyte cDNA expression library was citrullinated by PADI4 and was immunoscreened with anti-modified citrulline antibodies and sera from patients with rheumatoid arthritis. One immunoreactive cDNA clone containing a 2480-base pair insert was isolated and sequence analysis revealed that the cDNA included a part of the eukaryotic translation initiation factor 4G1. Immunoreactivity against a recombinant citrullinated eIF4G1 fragment was observed with high specificity in 50.0% of RA patients. The levels of antibodies against citrullinated eIF4G1 were correlated with those of anti-CCP antibodies. Citrullinated eIF4G1 was identified as a candidate citrullinated autoantigen in RA patients. Citrullination of eIF4G1 may thus be involved in the pathogenesis of RA.

Keywords: Autoantigen; Citrulline; Eukaryotic translation initiation factor; Peptidylarginine deiminase type 4; Rheumatoid arthritis

Rheumatoid arthritis (RA) is a common systemic autoimmune disease of unknown etiology characterized by synovial hyperplasia with inflammatory cell infiltration, which results in joint destruction. Numerous autoantibodies against a variety of autoantigens have been detected in sera from RA patients. However, many of these autoantibodies are not specific to RA. It was recently reported that antibodies directed against citrulline-containing proteins are highly specific to RA [1,2]. Citrulline is generated post-translationally from arginine by peptidylarginine deiminase (PADI). In a genomewide case-control study of single nucleotide polymorphisms, we reported that functional haplotypes of the gene encoding PADI4 were closely associated with RA and increased PADI4 mRNA stability probably resulting in increased protein citrullination and an increased chance of developing anti-citrullinated protein antibodies [3]. Several candidate citrullinated autoantigens, such as citrullinated fibrinogen [4] and citrullinated vimentin [5], were recently reported in RA. However, the role of these proteins in the pathogenesis of RA remains unknown.

To date, several candidate autoantigens have been identified in cartilage, including type II collagen [6,7], the cartilage proteoglycan component aggrecan [8], and human cartilage glycoprotein 39 [9]. Furthermore, cartilage has come under scrutiny because ubiquitous antigen glucose-6-phosphate isomerase, which is present on the cartilage surface, induces joint-specific autoimmune disease in the spontaneous mouse arthritis model K/BxN [10,11].

* Corresponding author. Fax: +81 3 5802 4803.
E-mail address: yamamoto-tky@umin.ac.jp (K. Yamamoto).

0006-291X/$ - see front matter © 2006 Elsevier Inc. All rights reserved.
doi:10.1016/j.bbrc.2005.12.160

In order to identify other citrullinated autoantigens involved in the pathogenesis of RA, we used RA sera and anti-modified citrulline antibodies to screen a human citrullinated chondrocyte cDNA expression library for targets of the autoimmune process in RA. Here, we report a novel citrullinated autoantigen, eukaryotic translation initiation factor 4G1 (eIF4G1) fragment, recognized specifically by sera from patients with RA. We further discuss the immunogenic features of the protein and its possible role as a substrate of PADI4.

Materials and methods

Human sera. Serum samples were obtained from a total of 100 patients with RA (84 females and 16 males; mean age: 61.1 years; range: 27–81 years). All patients satisfied the 1987 revised criteria of the American College of Rheumatology. A total of 34 serum samples were obtained from patients with other rheumatic diseases (29 females and 5 males; mean age: 43.5 years; range: 24–82 years), including systemic lupus erythematosus ($n = 18$), Sjögren's syndrome ($n = 4$), Churg–Strauss syndrome ($n = 2$), Behçet's disease ($n = 2$), polyarteritis nodosa ($n = 1$), systemic sclerosis ($n = 1$), mixed connective tissue disease ($n = 1$), polymyalgia rheumatica ($n = 1$), polymyositis/dermatomyositis ($n = 1$), anti-phospholipid syndrome ($n = 1$), pustulosis palmoplantaris ($n = 1$), and ulcerative colitis ($n = 1$). Patients were receiving treatment at the University of Tokyo Hospital. Written informed consent was obtained from all patients.

Control sera were obtained from 44 healthy donors (29 females and 15 males; mean age: 50.5 years; range: 23–78 years). All serum samples were stored at −20 °C until assay.

Immunological screening of cDNA libraries. Full-length human PADI4 cDNA was obtained by polymerase chain reaction using human bone marrow cDNA as a template [3] and was cloned into the prokaryotic expression vector pDEST17 (Invitrogen, San Diego, CA). His-tagged PADI4 was expressed in *Escherichia coli* BL21-SI (Invitrogen) by sodium chloride induction. Fusion protein was purified on a HiTrap column (Amersham Life Science, Cleveland, Ohio) according to the manufacturer's instructions. PADI activity was determined using *N*-benzoyl-L-arginine ethyl ester (BAEE, Sigma-Aldrich, St. Louis, MO) as a substrate, as described previously [12]. One unit of enzyme activity was defined as the activity required to produce 1 μmol of L-citrulline derivatives in 1 h at 37 °C.

XL1-Blue-MRF′ *E. coli* were infected with 1.5×10^4 plaque-forming units per plate (90 × 15 mm) of phage from the human chondrocyte lambda ZAP cDNA library following the manufacturer's instructions (Stratagene, La Jolla, CA). The resulting plaques were transferred onto nitrocellulose membranes treated with 20 mM isopropyl-1-thio-β-D-galactopyranoside (IPTG). Membranes were incubated with 1 unit of recombinant PADI4 overnight at 37 °C and were modified with 2, 3-butanedione monoxime and antipyrine in a strong acid solution (Upstate Biotechnology, Lake Placid, NY). The membranes were then incubated with rabbit polyclonal anti-modified citrulline antibody (Upstate). Horseradish peroxidase (HRP)-conjugated anti-rabbit antibodies (Upstate) were used as secondary antibodies and were visualized with enhanced chemiluminescence (ECL) reagents on Hyperfilm (Amersham). cDNA expression libraries were also screened with pooled sera of 5 patients with RA. Pooled sera of patients with RA were preadsorbed with *E. coli* lysate in order to reduce background sera activity. Immunoscreening was repeated using the same assay procedure until the positive phage reached clonality.

DNA sequencing and database searches. Positive phage clones were converted into phagemids by in vivo excision with the helper phage ExAssist and *E. coli* SOLR (Stratagene). Recombinant plasmids were then purified on Qiagen Maxi Prep columns (Qiagen) and were subjected to DNA sequencing. The cDNA inserts were sequenced on ABI3700 capillary sequencers (Applied Biosystems) using standard T3 forward and T7 reverse primers. cDNA sequences were subjected to a BLAST search of the genetic databases of the National Center for Biotechnology Information.

Expression and purification of recombinant fusion proteins. cDNA encoding the eIF4G1 fragment (2480 bp) was cloned into the expression vector pDEST17. *E. coli* BL21-SI transformed with this recombinant pDEST17 plasmid was grown at 30 °C, and sodium chloride was added in order to induce expression of recombinant protein. Fusion protein was purified on a column charged with Ni–NTA agarose (Qiagen).

Enzyme-linked immunosorbent assay. Each well of the microplates (Nunc, Rocester, NY) was coated with 100 μl of 5 μg/ml recombinant eIF4G1 fragment in carbonate buffer overnight at 4 °C. Wells were washed with Tris-buffered saline (TBS) and incubated for 3 h at 37 °C with 0.01 U/well of recombinant PADI4 or PADI4 in 50 mM EDTA in order to detect reactivity against citrullinated or uncitrullinated eIF4G1 fragment. Wells without recombinant protein were simultaneously prepared for non-specific background examination. To confirm citrullination of eIF4G1 fragment, wells were washed with Tris-buffered saline with 0.05% Tween 20 (TBS-T) and then incubated with 0.1% ovalbumin. The modified citrullinated eIF4G1 was detected by anti-modified citrulline antibody (Upstate) according to manufacturer's instruction. To detect anti-eIF4G1 or anti-citrullinated eIF4G1 antibodies in human sera, wells were washed with TBS-T, followed by blocking with 5% skim milk. Patients and control sera were diluted at 1:100 with TBS-T containing 5% skim milk and were preincubated with bacterial lysate in order to adsorb the reactivity to bacterial proteins. After reacting with coated recombinant proteins for 2 h at room temperature, wells were washed 4 times with TBS-T. Bound antibodies were incubated with horseradish peroxidase-conjugated goat $F(ab')_2$ anti-human IgG antibody (Biosource, Camarillo, CA) diluted at 1:50,000 and reacted with 3,3′,5,5′-tetramethylbenzidine (TMB) as a substrate. Sample optical density (OD) values were calculated as OD values for antigen-coated wells minus those for uncoated wells. Anti-CCP titers were determined using DIASTAT Anti-CCP Test (Axis-Shield Diagnostics, Dundee, Scotland, UK) according to manufacturer's instruction.

Immunoblotting. Recombinant eIF4G1 fragment (200 ng/lane) was incubated with 0.3 U of recombinant PADI4 overnight at 37 °C and was separated by electrophoresis on 10% SDS–polyacrylamide gels. Separated proteins were transferred onto a nitrocellulose membrane (Amersham), blocked with TBS-T containing 10% skim milk, and were incubated with goat anti-human eIF4G1 antibodies (Santa Cruz Biotechnology, Santa Cruz, CA) or serum samples, diluted at 1:100 in TBS-T with 5% skim milk-containing bacterial lysate. Horseradish peroxidase-conjugated rabbit anti-goat IgG (Santa Cruz Biotechnology) or goat $F(ab')_2$ anti-human IgG antibodies (Biosource) were used as secondary antibodies and were detected with ECL reagents (Amersham).

DNA extraction and genotyping. DNA from RA patients ($n = 39$) was extracted and PADI4 genotype was determined as described previously [3].

Statistical analysis. Statistical analysis was performed using Mann–Whitney *U* test, Pearson's correlation test, and χ^2 test. *p* values of less than 0.05 were considered to be statistically significant.

Results

Identification and expression of eIF4G1

Screening of the human citrullinated chondrocyte cDNA library identified a total of 13 clones. One of the clones reacted strongly with both anti-modified citrulline antibodies and RA pooled sera. The nucleotide sequence of this clone, which contained a 2480-bp insert, matched the 3′-region of the eIF4G1 sequence (5317 bp, GenBank Accession No. AY082886, Fig. 1A). The eIF4G1 fragment was cloned into the expression vector pDEST17 and was expressed as a His-tagged fusion protein. The purified

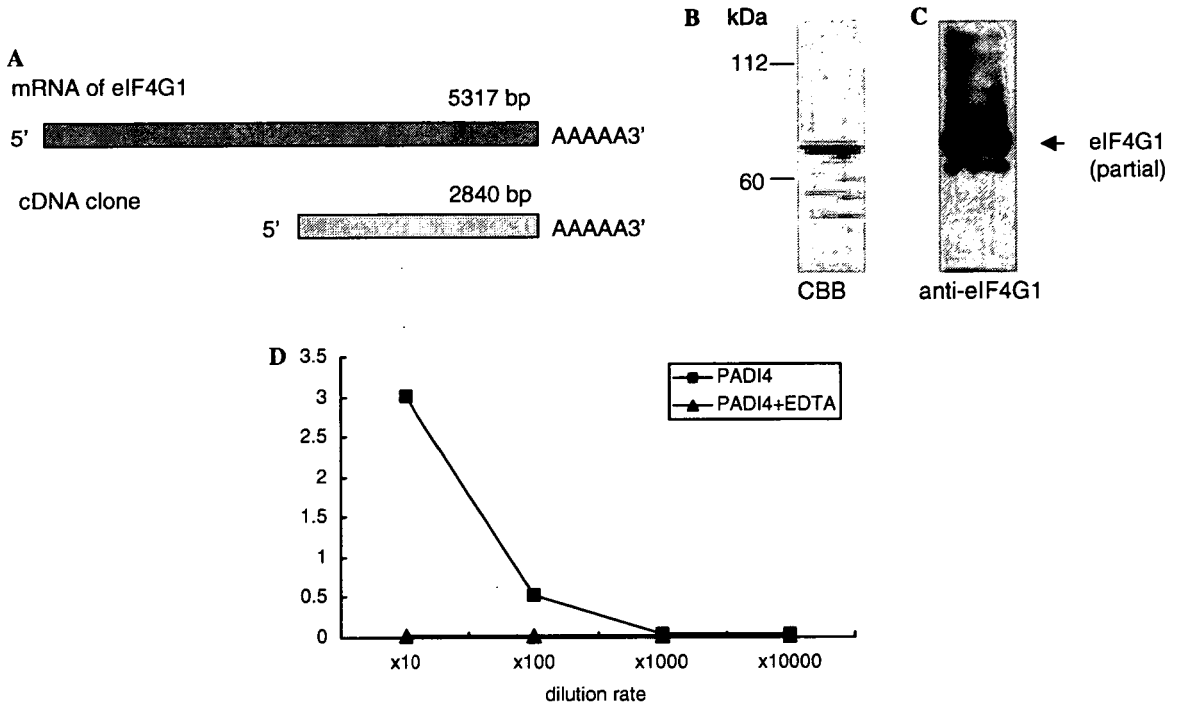

Fig. 1. Expression and immunoblotting of recombinant eIF4G1 fragment. (A) Insert of cDNA clone compared with the known eIF4G1 mRNA (bp, base pairs). (B) Purified recombinant eIF4G1 fragment was loaded onto 10% SDS–polyacrylamide gel and stained with Coomassie brilliant blue (CBB). (C) Separated proteins were transferred to nitrocellulose membrane, and immunoblotting using anti-eIF4G1 antibodies was performed. (D) Each dilution of recombinant eIF4G1 was incubated with PADI4 (■) or PADI4 in 50 mM EDTA (▲) and detected by anti-modified citrulline antibodies.

fusion protein had the expected molecular weight (Fig. 1B). Furthermore, immunoblotting confirmed that the recombinant eIF4G1 fragment reacted with anti-eIF4G1 antibodies (Fig. 1C). We also confirmed the citrullination of recombinant eIF4G1 fragment using ELISA (Fig. 1D).

Serum levels of antibodies against eIF4G1 and citrullinated eIF4G1

We used ELISA to investigate the prevalence of antibodies against uncitrullinated or citrullinated eIF4G1 fragment in patients with rheumatic diseases and in healthy individuals. As shown in Fig. 2, serum levels of IgG-type antibody against uncitrullinated eIF4G1 were higher in RA than in healthy controls ($p < 0.01$). Serum antibody levels against citrullinated eIF4G1 were also higher in RA than in controls ($p < 0.0001$) as well as in other rheumatic diseases ($p < 0.0001$). Anti-CCP antibody levels were also significantly higher in RA group than in healthy controls ($p < 0.0001$) or other rheumatic disease groups ($p < 0.0001$).

We defined the mean + 2SD value in control subjects as the cut-off value for anti-eIF4G1 or citrullinated eIF4G1 antibodies. The prevalence of anti-eIF4G1 antibodies in RA was 12.0%. After citrullination of eIF4G1, the prevalence of anti-citrullinated eIF4G1 increased to 50.0%. This percentage was significantly larger than those in controls and in other rheumatic diseases ($p < 0.001$, χ^2 test). All serum samples that were positive for anti-eIF4G1 were also positive for anti-citrullinated eIF4G1.

In RA, anti-citrullinated eIF4G1 antibody titers were significantly correlated with anti-cyclic citrullinated peptide (CCP) antibodies (Fig. 3). These results indicate that anti-citrullinated eIF4G1 antibodies are candidate citrullinated autoantigens in patients with RA.

Detection of antibodies against eIF4G1 and citrullinated eIF4G1 by immunoblotting

Positive serum samples were further examined by immunoblotting. We first confirmed that eIF4G1 was citrullinated by PADI4 using anti-modified citrulline antibodies. Of the 12 samples that were positive for anti-eIF4G fragment by ELISA, 9 were confirmed to recognize eIF4G1 fragment. Of the 50 samples that were positive for anti-citrullinated eIF4G1 by ELISA, 48 reacted to citrullinated eIF4G1. Representative results are shown in Fig. 4. Some RA sera also reacted with recombinant PADI4. These results agree with our previous findings that antibodies against PADI4 are present in RA patients [13].

Relationship between PADI4 haplotype and antibody against citrullinated eIF4G1

Table 1 shows the relationship between PADI4 haplotype and the presence of antibodies against citrullinated eIF4G1 or CCP in sera from patients with RA. Patients who were positive for antibody against citrullinated eIF4G1 were more likely to possess the susceptible allele (59.5%) than patients who were negative for antibody

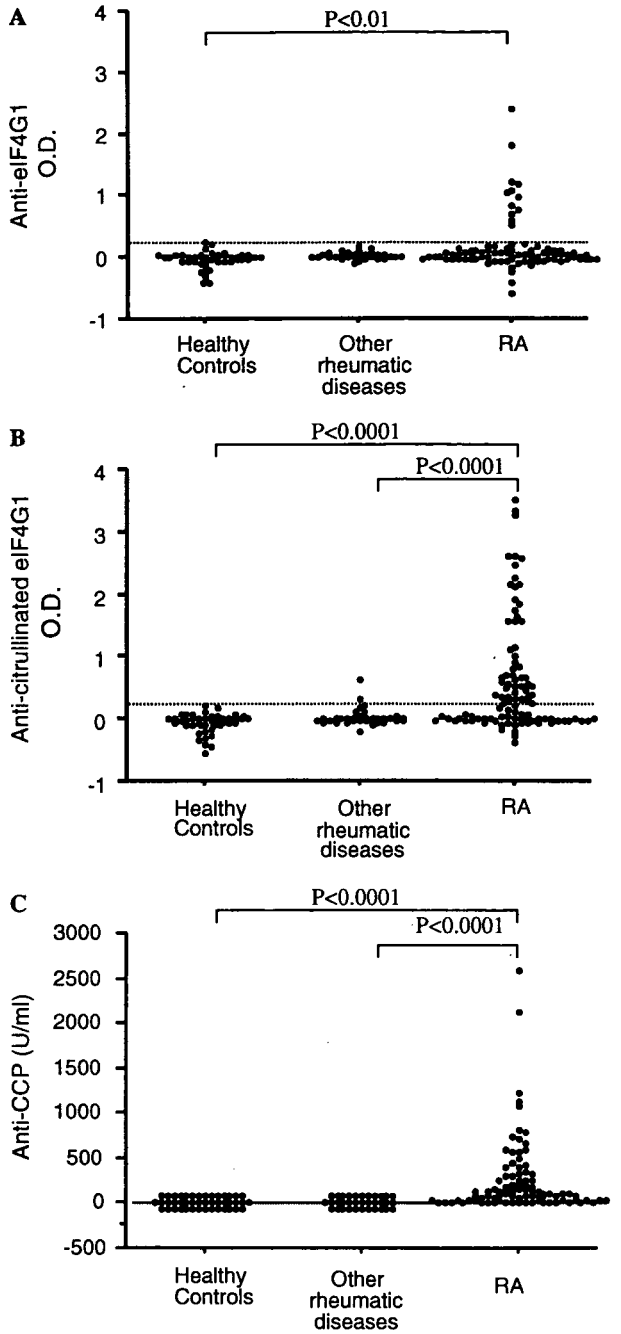

Fig. 2. Presence of autoantibodies against recombinant eIF4G1 fragment (A), citrullinated eIF4G1 fragment (B), and CCP (C) in sera from patients with RA, other rheumatic diseases, and healthy controls. Patient and control sera were diluted at 1:100. Dotted line represents cut-off value, which was calculated as the mean OD + 2SD in control subjects.

against citrullinated eIF4G1 (36.1%, $p = 0.03$, χ^2 test). On the other hand, the relationship between PADI4 haplotype and anti-CCP antibody was not significant ($p = 0.47$, χ^2 test).

Discussion

We identified citrullinated eIF4G1 fragment as a novel RA-specific autoantigen by immunoscreening a human chondrocyte cDNA expression library. eIF4G is a translational initiation factor and is recognized as the central organizing protein in recruitment of 43S preinitiation complex to mRNA [14]. There are two isoforms of eIF4G in mammals: eIF4G1 and eIF4G2. eIF4G1 is associated with two other factors, the cap-binding protein eIF4E and the RNA helicase eIF4A, in the large protein complex eIF4F [14]. Previous studies have shown that antibodies against eIF4G1 were present in a patient with squamous cell lung carcinoma [15]. However, the involvement of eIF4G1 or citrullinated eIF4G1 in the pathogenesis of RA is not certain.

RA is accompanied by the generation of numerous autoantibodies in the serum of patients. Although most of these autoantibodies are not specific to RA, autoantibodies against citrullinated proteins are reported to be highly specific for RA [1]. Candidate citrullinated autoantigens recognized in RA sera are filaggrin [16], keratin [17], vimentin [5], and fibrinogen or fibrin [4], but the true autoantigens in RA are unknown. This prompted research into other candidate citrullinated autoantigens.

Citrullination is mediated by PADI, a calcium-dependent enzyme that catalyzes the post-translational conversion of arginine residues to citrulline. There are five isoforms of PADI [18] and PADI4 is reported to be particularly important in RA [3]. Citrullination by PADI4 may play a critical role in breaking tolerance of RA by altering the antigenicity of native self-peptides. Therefore, we selected a cDNA expression library of proteins citrullinated by PADI4. In addition, this method enabled detection of trace or insoluble autoantigens.

Using the recombinant eIF4G1 fragment, we found that the mean sensitivity of the ELISA was 50.0%, with 97.4% specificity and 96.2% positive predictive value. The specificity and positive predictive value of this assay were comparable to those of the CCP-assay [19,20]. Of the anti-citrullinated eIF4G1-positive RA sera, most of them were positive for anti-CCP. Furthermore, anti-citrullinated eIF4G1 antibody titers were significantly correlated with anti-CCP antibody titers. This correlation suggests that anti-citrullinated eIF4G1 antibodies compose a subset of anti-CCP antibodies. It has been reported that antibodies against citrullinated proteins are heterogeneous [1]. Antibodies against citrullinated eIF4G1 may thus be one of several antibodies directed against citrullinated proteins.

Three samples that were positive for anti-eIF4G1 and two samples that were positive for anti-citrullinated eIF4G1 by ELISA did not recognize eIF4G1 or citrullinated eIF4G1 by immunoblotting. In these cases, antibodies may target conformational epitopes of eIF4G1.

It was recently reported that PADI4 regulated histone arginine methylation by converting methyl-arginine to citrulline, thus affecting chromatin structure [21,22]. In a similar way, PADI4 may catalyze other molecules, such as eIF4G1, under physiological conditions. Because PADI4 enzyme needs high calcium ion concentration for its enzyme activity [23], citrullination is reported to occur

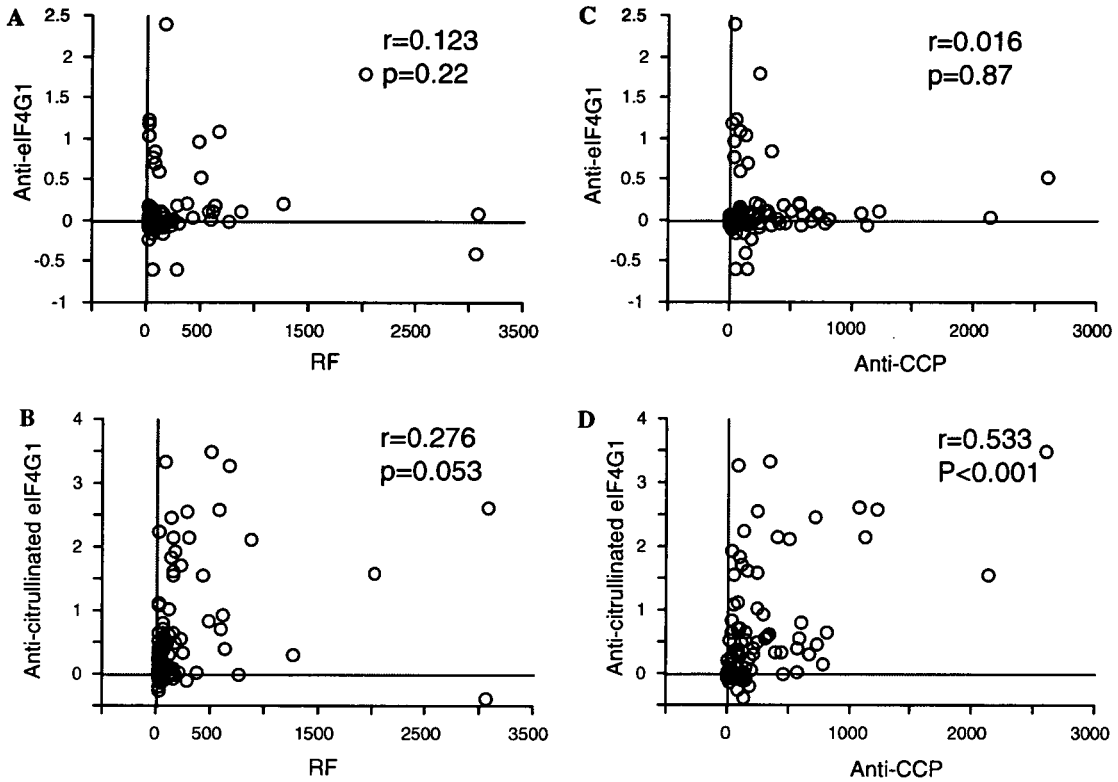

Fig. 3. Correlation between disease markers and anti-eIF4G1 or anti-citrullinated eIF4G1 antibody titer in patients with RA. Correlation between RF levels and anti-eIF4G1 (A) or anti-citrullinated eIF4G1 (B) levels. Correlation between anti-CCP levels and anti-eIF4G1 (C) or anti-citrullinated eIF4G1 (D) levels. Correlation coefficient (r) and p value are shown.

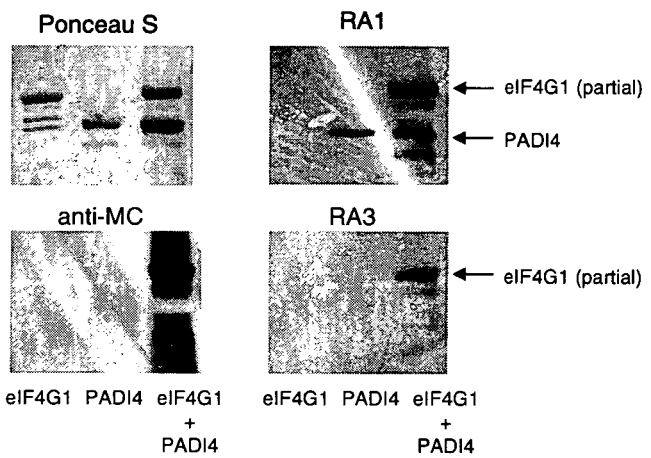

Fig. 4. Immunoreactivity of uncitrullinated or citrullinated eIF4G1. Recombinant eIF4G1 fragment in the presence or absence of PADI4 was separated by 10% SDS-PAGE and was transferred onto nitrocellulose membranes. Serum samples that were positive for anti-citrullinated eIF4G1 on ELISA were examined by immunoblotting. Control membranes were stained with Ponceau S. Citrullination of eIF4G1 fragment by PADI4 was confirmed using anti-modified citrulline antibodies. RA1, RA3: RA patient sera. Representative samples are shown.

Table 1
Association between PADI4 haplotype and antibody to citrullinated eIF4G1 or CCP

	PADI4 susceptible allele	PADI4 non-susceptible allele
Anti-citrullinated eIF4G1		
Positive	25	17
Negative	13	23
Anti-CCP		
Positive	33	37
Negative	5	3

during apoptosis [24,25]. Apoptosis induces degradation or modification of various proteins and the generation of new epitopes. If these proteins are cleared incorrectly, they could break tolerance by epitope spreading and this may trigger specific autoimmune responses [26]. eIF4G1 is reported to be cleaved by caspase 3 during the early stages of apoptosis [27]. Furthermore, our results showed that antibodies against uncitrullinated eIF4G1 were present in 12% of RA serum samples, which suggests that epitope spreading to uncitrullinated regions of eIF4G1 has occurred. In fact, all serum samples that recognized uncitrullinated eIF4G1 were positive for anti-citrullinated eIF4G1, indicating reactive epitopes spread from epitopes around the citrullinated regions to uncitrullinated parts of the molecule. Citrullinated eIF4G1 might play an important role in triggering autoimmunity in RA. To determine the independence of antigenicity of each antigen, we have done affinity purification and absorbing experiment

according to the method of Olmsted [28]. Serum absorbed with eIF4G1 showed higher titer of citrullinated eIF4G1 than that of eIF4G1, and affinity purified anti-eIF4G1 showed higher titer of eIF4G1 than that of citrullinated eIF4G1 (data not shown). However, as to the affinity purification and absorbing experiments using citrullinated eIF4G1, we could not show the independence of the antigenicity, probably because of the small amount of anti-citrullinated eIF4G1 antibodies in the patients' sera. Taken together, we can suggest that at least a part of patient's sera recognized different epitopes of eIF4G1 and citrullinated eIF4G1, according to our additional experiments. However, it is difficult to determine the overlapping of epitopes. Further investigation is needed whether citrullination of eIF4G1 occurs in vivo and citrullinated eIF4G1 actually contributes to breaking immunological tolerance.

We expressed only a portion of eIF4G1 and investigated its antigenicity in this experiment. The antigenicity of eIF4G1 or citrullinated eIF4G1 using full-length protein should be examined in the future. Recombinant eIF4G1 fragment contained 58 arginine residues, and it is uncertain which arginine residues are citrullinated in the recombinant protein. Further study is needed in order to identify which citrulline residues are important for antigenicity of epitopes in RA.

With regard to the association between PADI4 haplotype and the presence of antibodies against citrullinated eIF4G1, despite the small number, patients who were positive for antibodies against citrullinated eIF4G1 tended to possess a susceptible PADI4 allele. These findings indicate that PADI4 mRNA stability affects the generation of anti-citrullinated eIF4G1 antibodies and suggests the contribution of citrullinated eIF4G1 to the pathophysiology of RA.

In summary, we demonstrated that citrullinated eIF4G1 is a candidate autoantigen in RA patients. Our results show that citrullination of eIF4G1 may be involved in the pathogenesis of RA.

Acknowledgments

This work was supported by a grant from the Japanese Millennium Project. We thank Dr. Hitoshi Okazaki for helpful discussion and review of the manuscript.

References

[1] G.A. Schellekens, B.A. de Jong, F.H. van den Hoogen, L.B. van de Putte, W.J. van Venrooij, Citrulline is an essential constituent of antigenic determinants recognized by rheumatoid arthritis-specific autoantibodies, J. Clin. Invest. 101 (1998) 273–281.

[2] E. Girbal-Neuhauser, J.J. Durieux, M. Arnaud, P. Dalbon, M. Sebbag, C. Vincent, M. Simon, T. Senshu, C. Masson-Bessiere, C. Jolivet-Reynaud, M. Jolivet, G. Serre, The epitopes targeted by the rheumatoid arthritis-associated antifilaggrin autoantibodies are post-translationally generated on various sites of (pro)filaggrin by deimination of arginine residues, J. Immunol. 162 (1999) 585–594.

[3] A. Suzuki, R. Yamada, X. Chang, S. Tokuhiro, T. Sawada, M. Suzuki, M. Nagasaki, M. Nakayama-Hamada, R. Kawaida, M. Ono, M. Ohtsuki, H. Furukawa, S. Yoshino, M. Yukioka, S. Tohma, T. Matsubara, S. Wakitani, R. Teshima, Y. Nishioka, A. Sekine, A. Iida, A. Takahashi, T. Tsunoda, Y. Nakamura, K. Yamamoto, Functional haplotypes of PADI4, encoding citrullinating enzyme peptidylarginine deiminase4, are associated with rheumatoid arthritis, Nat. Genet. 34 (2003) 395–402.

[4] C. Masson-Bessiere, M. Sebbag, E. Girbal-Neuhauser, L. Nogueira, C. Vincent, T. Senshu, G. Serre, The major synovial targets of the rheumatoid arthritis-specific antifilaggrin autoantibodies are deiminated forms of the alpha- and beta-chains of fibrin, J. Immunol. 166 (2001) 4177–4184.

[5] E.R. Vossenaar, N. Despres, E. Lapointe, A. van der Heijden, M. Lora, T. Senshu, W.J. van Venrooij, H.A. Menard, Rheumatoid arthritis specific anti-Sa antibodies target citrullinated vimentin, Arthritis Res. Ther. 6 (2004) R142–R150.

[6] J. Ronnelid, J. Lysholm, A. Engstrom-Laurent, L. Klareskog, B. Heyman, Local anti-type II collagen antibody production in rheumatoid arthritis synovial fluid. Evidence for an HLA-DR4-restricted IgG response, Arthritis Rheum. 37 (1994) 1023–1029.

[7] A. Tarkowski, L. Klareskog, H. Carlsten, P. Herberts, W.J. Koopman, Secretion of antibodies to types I and II collagen by synovial tissue cells in patients with rheumatoid arthritis, Arthritis Rheum. 32 (1989) 1087–1092.

[8] N.J. Goodstone, M.C. Doran, R.N. Hobbs, R.C. Butler, J.J. Dixey, B.A. Ashton, Cellular immunity to cartilage aggrecan core protein in patients with rheumatoid arthritis and non-arthritic controls, Ann. Rheum. Dis. 55 (1996) 40–46.

[9] G.F. Verheijden, A.W. Rijnders, E. Bos, C.J. Coenen-de Roo, C.J. van Staveren, A.M. Miltenburg, J.H. Meijerink, D. Elewaut, F. de Keyser, E. Veys, A.M. Boots, Human cartilage glycoprotein-39 as a candidate autoantigen in rheumatoid arthritis, Arthritis Rheum. 40 (1997) 1115–1125.

[10] I. Matsumoto, M. Maccioni, D.M. Lee, M. Maurice, B. Simmons, M. Brenner, D. Mathis, C. Benoist, How antibodies to a ubiquitous cytoplasmic enzyme may provoke joint-specific autoimmune disease, Nat. Immunol. 3 (2002) 360–365.

[11] B.T. Wipke, Z. Wang, J. Kim, T.J. McCarthy, P.M. Allen, Dynamic visualization of a joint-specific autoimmune response through positron emission tomography, Nat. Immunol. 3 (2002) 366–372.

[12] K. Watanabe, K. Akiyama, K. Hikichi, R. Ohtsuka, A. Okuyama, T. Senshu, Combined biochemical and immunochemical comparison of peptidylarginine deiminases present in various tissues, Biochim. Biophys. Acta 966 (1988) 375–383.

[13] Y. Takizawa, T. Sawada, A. Suzuki, R. Yamada, T. Inoue, K. Yamamoto, Peptidylarginine deiminase 4 (PADI4) identified as a conformation-dependent autoantigen in rheumatoid arthritis, Scand. J. Rheumatol. 34 (2005) 212–215.

[14] M. Holcik, N. Sonenberg, R.G. Korneluk, Internal ribosome initiation of translation and the control of cell death, Trends Genet. 16 (2000) 469–473.

[15] C. Bauer, I. Diesinger, N. Brass, H. Steinhart, H. Iro, E.U. Meese, Translation initiation factor eIF-4G is immunogenic, overexpressed, and amplified in patients with squamous cell lung carcinoma, Cancer 92 (2001) 822–829.

[16] M. Sebbag, M. Simon, C. Vincent, C. Masson-Bessiere, E. Girbal, J.J. Durieux, G. Serre, The antiperinuclear factor and the so-called antikeratin antibodies are the same rheumatoid arthritis-specific autoantibodies, J. Clin. Invest. 95 (1995) 2672–2679.

[17] B.J. Young, R.K. Mallya, R.D. Leslie, C.J. Clark, T.J. Hamblin, Anti-keratin antibodies in rheumatoid arthritis, Br. Med. J. 2 (1979) 97–99.

[18] E.R. Vossenaar, A.J. Zendman, W.J. van Venrooij, G.J. Pruijn, PAD, a growing family of citrullinating enzymes: genes, features and involvement in disease, Bioessays 25 (2003) 1106–1118.

[19] W.J. van Venrooij, J.M. Hazes, H. Visser, Anticitrullinated protein/peptide antibody and its role in the diagnosis and prognosis of early rheumatoid arthritis, Neth. J. Med. 60 (2002) 383–388.

[20] K. Suzuki, T. Sawada, A. Murakami, T. Matsui, S. Tohma, K. Nakazono, M. Takemura, Y. Takasaki, T. Mimori, K. Yamamoto,

High diagnostic performance of ELISA detection of antibodies to citrullinated antigens in rheumatoid arthritis, Scand. J. Rheumatol. 32 (2003) 197–204.

[21] Y. Wang, J. Wysocka, J. Sayegh, Y.H. Lee, J.R. Perlin, L. Leonelli, L.S. Sonbuchner, C.H. McDonald, R.G. Cook, Y. Dou, R.G. Roeder, S. Clarke, M.R. Stallcup, C.D. Allis, S.A. Coonrod, Human PAD4 regulates histone arginine methylation levels via demethylimination, Science 306 (2004) 279–283.

[22] G.L. Cuthbert, S. Daujat, A.W. Snowden, H. Erdjument-Bromage, T. Hagiwara, M. Yamada, R. Schneider, P.D. Gregory, P. Tempst, A.J. Bannister, T. Kouzarides, Histone deimination antagonizes arginine methylation, Cell 118 (2004) 545–553.

[23] M. Inagaki, H. Takahara, Y. Nishi, K. Sugawara, C. Sato, Ca^{2+}-dependent deimination-induced disassembly of intermediate filaments involves specific modification of the amino-terminal head domain, J. Biol. Chem. 264 (1989) 18119–18127.

[24] H. Asaga, M. Yamada, T. Senshu, Selective deimination of vimentin in calcium ionophore-induced apoptosis of mouse peritoneal macrophages, Biochem. Biophys. Res. Commun. 243 (1998) 641–646.

[25] M. Mizoguchi, M. Manabe, Y. Kawamura, Y. Kondo, K. Ishidoh, E. Kominami, K. Watanabe, H. Asaga, T. Senshu, H. Ogawa, Deimination of 70-kDa nuclear protein during epidermal apoptotic events in vitro, J. Histochem. Cytochem. 46 (1998) 1303–1309.

[26] R.J. Rodenburg, J.M. Raats, G.J. Pruijn, W.J. van Venrooij, Cell death: a trigger of autoimmunity? Bioessays 22 (2000) 627–636.

[27] M.J. Clemens, M. Bushell, S.J. Morley, Degradation of eukaryotic polypeptide chain initiation factor (eIF) 4G in response to induction of apoptosis in human lymphoma cell lines, Oncogene 17 (1998) 2921–2931.

[28] J.B. Olmsted, Affinity purification of antibodies from diazotized paper blots of heterogeneous protein samples, J. Biol. Chem. 256 (1981) 11955–11957.

nature genetics

A functional variant in *FCRL3*, encoding Fc receptor-like 3, is associated with rheumatoid arthritis and several autoimmunities

Yuta Kochi[1,2], Ryo Yamada[1], Akari Suzuki[1], John B Harley[3], Senji Shirasawa[4], Tetsuji Sawada[2], Sang-Cheol Bae[5], Shinya Tokuhiro[1], Xiaotian Chang[1], Akihiro Sekine[6], Atsushi Takahashi[7], Tatsuhiko Tsunoda[7], Yozo Ohnishi[8], Kenneth M Kaufman[3], Changsoo Paul Kang[9], Changwon Kang[9], Shigeru Otsubo[10], Wako Yumura[11], Akio Mimori[4], Takao Koike[12], Yusuke Nakamura[10,13], Takehiko Sasazuki[4] & Kazuhiko Yamamoto[1,2]

Rheumatoid arthritis is a common autoimmune disease with a complex genetic etiology. Here we identify a SNP in the promoter region of *FCRL3*, a member of the Fc receptor-like family, that is associated with susceptibility to rheumatoid arthritis (odds ratio = 2.15, $P = 0.00000085$). This polymorphism alters the binding affinity of nuclear factor-κB and regulates *FCRL3* expression. We observed high *FCRL3* expression on B cells and augmented autoantibody production in individuals with the disease-susceptible genotype. We also found associations between the SNP and susceptibility to autoimmune thyroid disease and systemic lupus erythematosus. *FCRL3* may therefore have a pivotal role in autoimmunity.

Rheumatoid arthritis is one of the most common autoimmune diseases and is characterized by inflammation of synovial tissue and joint destruction. Although the disease is believed to result from a combination of genetic and environmental factors, its complete etiology has not yet been clarified[1]. Specific haplotypes of human leukocyte antigen (HLA)-DRB1, usually referred to as shared-epitope sequences[2], have been repeatedly reported to confer susceptibility to rheumatoid arthritis[3,4]; other genetic components are also involved[5]. This combination of HLA haplotypes and non-HLA genes accounting for disease susceptibility is also observed for other autoimmune diseases[6–8]. In autoimmune thyroid disease (AITD), for instance, the *HLA-DR3* haplotype is associated with disease risk, as is a functional haplotype of a non-HLA gene, *CTLA4*, that has recently been associated with AITD susceptibility[9].

Identification of non-HLA genes associated with rheumatoid arthritis susceptibility and other autoimmunities seems difficult, because of the low relative risk of disease resulting from these non-HLA genes compared with the strong relative risk from disease-associated HLA haplotypes. In a search for non-HLA determinants of disease susceptibility, whole-genome studies have been done for both human autoimmune diseases and experimental animal models. These studies have identified nonrandom clustering of susceptibility loci for clinically distinct diseases[8,10]. The overlap of susceptibility loci for multiple autoimmunities suggests that common susceptibility genes exist in those regions. Intense studies of loci-clustering regions identified genes commonly associated with multiple autoimmune diseases, such as *CTLA4* on 2q33 (ref. 9), *SLC22A4* and *SLC22A5* on 5q31 (ref. 11) and *PTPN22* on 1p13 (ref. 12).

Cytoband 1q21–23 is one of the regions implicated in susceptibility to multiple autoimmune diseases. The Fcγ receptor (FcγR) II/III genes are located at 1q23, and a new family of genes, Fc receptor-like genes (FCRLs, also known as FcRHs[13,14], IRTAs[15,16] or SPAPs[17]), clusters nearby at 1q21 (**Fig. 1a**). FCRLs have high structural homology with classical FcγRs, although their ligands and function are not yet known. These receptors are good candidates for involvement in autoimmunity, as they are believed to be involved in the pathogenesis of rheumatoid arthritis and other autoimmune diseases[18]. Region 1q23 is a candidate locus for susceptibility to systemic lupus erythematosus

[1]Laboratory for Rheumatic Diseases, SNP Research Center, RIKEN, Yokohama 230-0045, Japan. [2]Department of Allergy and Rheumatology, Graduate School of Medicine, the University of Tokyo, Tokyo 113-0033, Japan. [3]University of Oklahoma; US Department of Veterans Affairs; and Oklahoma Medical Research Foundation, Oklahoma City, Oklahoma 73104, USA. [4]International Medical Center of Japan, Tokyo 162-8655, Japan. [5]Department of Internal Medicine, Division of Rheumatology, the Hospital for Rheumatic Diseases, Hanyang University, Seoul 133-792, Republic of Korea. Laboratories for [6]Genotyping, [7]Medical Informatics and [8]SNP Analysis, SNP Research Center, RIKEN, Yokohama 230-0045, Japan. [9]Department of Biological Sciences, Korea Advanced Institute of Science and Technology, Daejeon 305-701, Republic of Korea. [10]Laboratory of Molecular Medicine, Human Genome Center, Institute of Medical Science, the University of Tokyo, Tokyo 108-8639, Japan. [11]Department of Medicine, Kidney Center, Tokyo Women's Medical University, Tokyo 162-8666, Japan. [12]Department of Medicine II, Hokkaido University School of Medicine, Sapporo 060-8638, Japan. [13]Research Group for Personalized Medicine, SNP Research Center, RIKEN, Yokohama 230-0045, Japan. Correspondence should be addressed to R.Y. (ryamada@src.riken.go.jp).

Published online 17 April 2005; doi:10.1038/ng1540

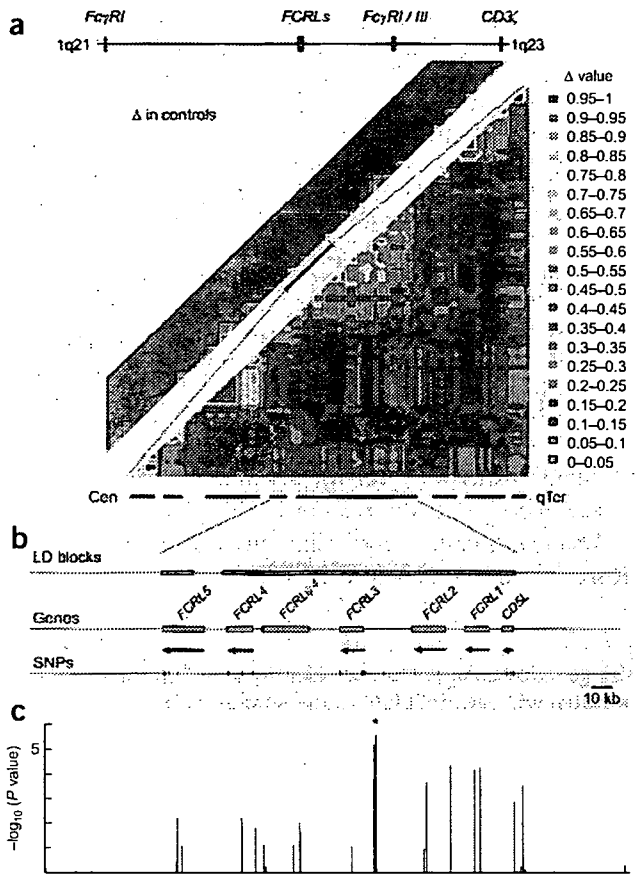

Figure 1 LD and association of the FCRL gene cluster. (**a**) Pairwise LD between SNPs, as measured by Δ in 658 controls. The 16-Mb region in 1q21–23 (upper left) and the 2-Mb region around the FCRL gene cluster (lower right) were evaluated. (**b**) Location of LD blocks, genes and 41 SNPs in the FCRL gene cluster. (**c**) Case-control association test with 41 SNPs in the FCRL gene cluster using 830 affected individuals and 658 controls. *Peak association.

(SLE), and variants in the classical FcγR II/III genes partially account for disease susceptibility[6,19]. Region 1q21 is a candidate locus for susceptibility to psoriasis (*PSORS4*; refs. 7,20) and multiple sclerosis[21]. The mouse homologous region to human 1q21, on chromosome 3, also contains susceptibility loci for multiple autoimmune disease models[8], including collagen-induced arthritis (*Cia5*, also called *Mcia2* (ref. 22); *Eae3* (ref. 23); *Tmevd2* (ref. 24); *Idd10*; and *Idd17* (ref. 25)). Although 1q21–23 is a good candidate region for containing rheumatoid arthritis–susceptibility genes, the association of classical FcγRs with disease susceptibility remains controversial[26,27]. Here we focused on the 1q21–23 region to identify rheumatoid arthritis–associated genes in Japanese subjects using linkage disequilibrium (LD) mapping.

RESULTS

Case-control study by SNP-based LD mapping at 1q21–23

To evaluate the extent of association, we analyzed LD with SNPs distributed in a 16-Mb region on 1q21–23, including the FCRL gene cluster and the classical FcγRs (**Fig. 1a**). We genotyped 658 control subjects for 742 SNPs from the JSNP database and selected 491 SNPs with allele frequency > 0.1, successful genotyping rate > 0.95 and P > 0.01 with Hardy-Weinberg equilibrium testing for evaluation of LD. We calculated the pairwise LD index Δ (ref. 28) for each pair of SNPs, identifying 110 LD blocks[11] at a threshold of Δ > 0.5 (**Fig. 1a**).

For association testing, we examined the Japanese set of 830 cases and 658 controls used for LD block evaluation. We initially genotyped 94 rheumatoid arthritis cases for 491 SNPs and compared their allele frequencies with those of 658 control subjects. We identified nine SNPs that had allele frequencies differing by more than 0.1 between 658 controls and 94 cases with $P < 0.01$. We genotyped the remaining cases for these nine SNPs and tested their allele frequencies for case-control association. We identified the smallest P value between an intronic SNP in the gene *FCRL3* and rheumatoid arthritis (fcrl3_6, $P = 1.8 \times 10^{-5}$; association was statistically significant in both rheumatoid arthritis subgroups (94 and 736 individuals)). This SNP was located in a LD block containing four of the five FCRL genes; the fifth was in the adjacent block. We therefore evaluated the origin of this association in these two LD blocks (**Fig. 1b**), although our results do not exclude the presence of variants associated with rheumatoid arthritis or other autoimmune diseases in other LD blocks at 1q21–23.

In addition to the 25 SNPs of the 491 that we used for LD block evaluation, we identified 16 additional SNPs in exons and 5′ and 3′ flanking regions of five FCRL genes and one pseudogene (*FCRLψ4*) by searching the public database and sequencing genomic DNA from Japanese individuals with rheumatoid arthritis. We genotyped these 16 SNPs in the identical case and control samples (830 cases, 658 controls) to increase the density of variants in the targeted region. We observed a peak of association in a short segment consisting of four SNPs in *FCRL3* ($P < 1.0 \times 10^{-4}$; **Fig. 1c** and **Supplementary Table 1** online): fcrl3_3, fcrl3_4, fcrl3_5 and fcrl3_6, located at nt −169, −110, +358 (5′ untranslated region of exon 2) and +1381 (intron 3; 204 bp and 859 bp from the 3′ and 5′ ends of the flanking exons) relative to the transcription initiation site, respectively.

We observed the smallest P value without correction in recessive-trait genotype comparison of fcrl3_3 in *FCRL3* ($P = 8.5 \times 10^{-7}$; odds ratio = 2.15; 95% confidence interval = 1.58–2.93; **Table 1**). This

Table 1 Case-control analysis of *FCRL3*

			Allele 1 frequency		Genotype 11 versus 12 + 22		
SNP	Location	Allele (1/2)	Affected individuals	Controls	OR (95% c.i.)	χ^2	P
fcrl3_3	−169	C/T	0.42	0.35	2.15 (1.58–2.93)	24.3	0.00000085
fcrl3_4	−110	A/G	0.25	0.18	3.01 (1.71–5.29)	16.1	0.000060
fcrl3_5	Exon 2	C/G	0.42	0.35	2.05 (1.51–2.78)	21.6	0.0000033
fcrl3_6	Intron 3	A/G	0.42	0.34	2.02 (1.49–2.75)	20.8	0.0000052

SNPs with $P < 0.0001$ in allele frequency comparison test are shown. c.i., confidence interval; OR, odds ratio.

Table 2 Haplotype structure and frequency in *FCRL3*

Haplotype	Sequence (fcrl3_3-4-5-6)	Frequency	
		Affected individuals	Controls
1	TGGG	0.58	0.65
2	CACA	0.25	0.19
3	CGCA	0.17	0.14

Haplotypes with frequency >0.01 are shown.

P value was still significant when the most conservative Bonferroni correction was applied (comparisons for 507 SNPs; corrected $P = 0.00043$). The four strongly associated SNPs were in LD with each other, and we inferred three common haplotypes (**Table 2**); fcrl3_3, fcrl3_5 and fcrl3_6 showed strong LD with each other ($\Delta > 0.99$), whereas fcrl3_4 showed relatively weak LD with the other three SNPs (mean $\Delta = 0.68$).

To identify causal variants in this segment on the basis of genotype data, we carried out a forward stepwise-regression procedure with a cut-off *P* value to proceed to the next step of 0.01 (ref. 29). No SNP in FCRL genes other than *FCRL3* improved the model. None of the four SNPs in *FCRL3* were preferred over the others in these data (data not shown). This result implied that one of the SNPs in *FCRL3* might cause the disease, but the possibility remained that variants in other genes were truly associated with the disease.

To validate the case-control association test, we evaluated the impact of population stratification on the case-control study (830 cases, 658 controls). We selected 2,069 SNPs, each of which was identified as a tagging SNP[30] in 2,069 distinct LD segments that were previously identified by genotyping 74,842 SNPs distributed in autosomal chromosomes[31]. We analyzed population structure[32] and the χ^2 sum[33] to evaluate stratification but detected no significant evidence of population stratification (**Supplementary Fig. 1** online). These results are suggestive of no or negligible stratification of our samples and support the validity of the case-control association results by removing this confounding factor from further consideration.

Regulatory effect of SNP −169C→T on *FCRL3* expression

Because none of the four SNPs in *FCRL3* (fcrl3_3, fcrl3_4, fcrl3_5 and fcrl3_6) produces amino-acid substitutions, we assessed potential effects of the SNPs on transcription factor binding using TRANSFAC software. Nuclear factor-κB (NF-κB) was predicted to bind the sequence containing the rheumatoid arthritis–susceptibility allele fcrl3_3 (−169C) with a high score (core match 1.000, matrix match 0.957); substitution with the nonsusceptible allele T decreased the score of NF-κB binding substantially (core match 0.760, matrix match 0.824). The other three SNPs were not predicted to bind to any transcriptional factor with high score, and nucleotide substitution was not predicted to affect binding at any regulatory factor. We therefore focused on the 5′ flanking region of fcrl3_3 to explore the regulatory effects on expression of *FCRL3*.

We carried out reporter gene analysis using the genomic sequence of *FCRL3* from nt −523 to +203. We made constructs corresponding to the three haplotypes using SNPs at nt −169 (C→T, fcrl3_3) and −110 (G→A, fcrl3_4; **Fig. 2a**) and used them to transfect Raji cells, a Burkitt's lymphoma cell line that expresses *FCRL3* (ref. 13) and is derived from germinal center B cells. Luciferase activity was substantially greater in cells transfected with −169C −110G or −169C −110A constructs than in cells transfected with −169T −110G constructs. This suggests that SNP −169C→T is crucial for regulation of *FCRL3* expression. To clarify, we cloned single or four tandem copies of 30-bp

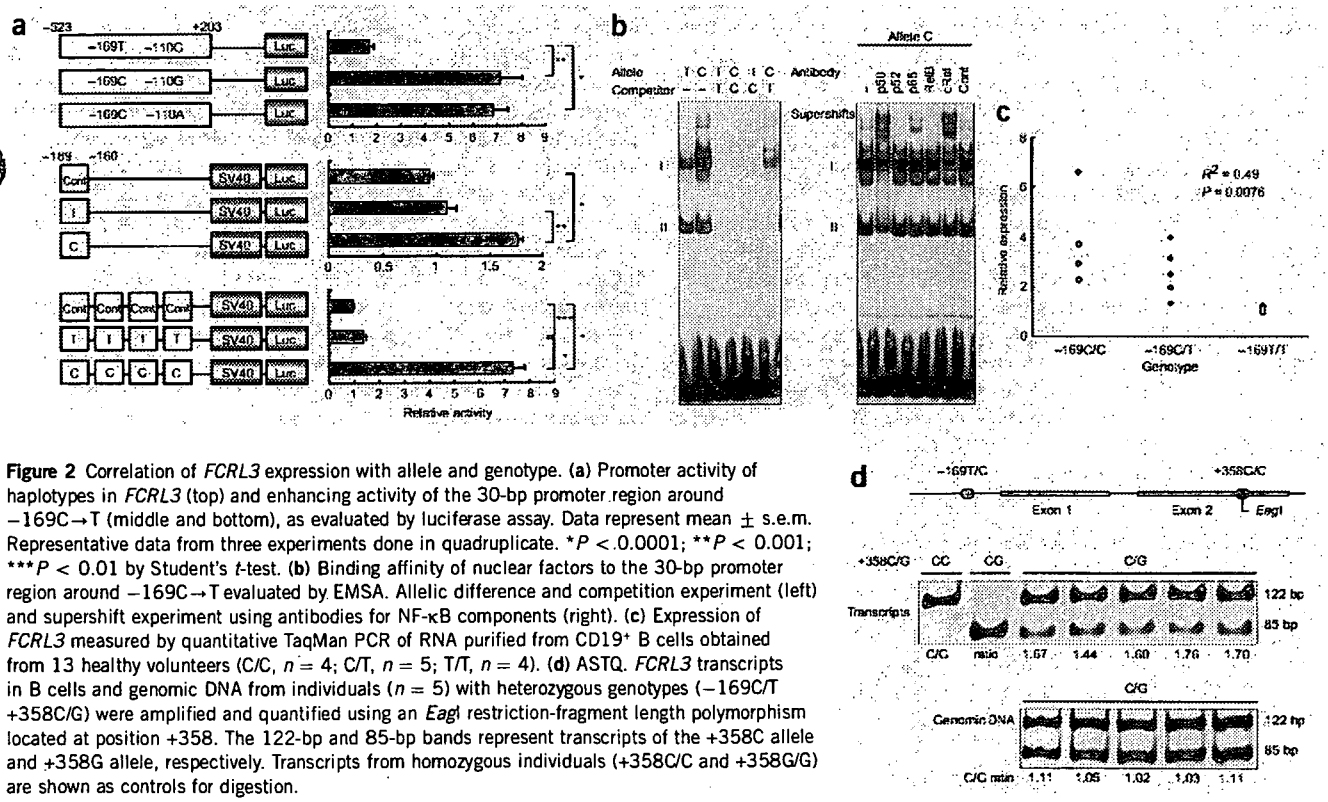

Figure 2 Correlation of *FCRL3* expression with allele and genotype. (**a**) Promoter activity of haplotypes in *FCRL3* (top) and enhancing activity of the 30-bp promoter region around −169C→T (middle and bottom), as evaluated by luciferase assay. Data represent mean ± s.e.m. Representative data from three experiments done in quadruplicate. $^*P < 0.0001$; $^{**}P < 0.001$; $^{***}P < 0.01$ by Student's *t*-test. (**b**) Binding affinity of nuclear factors to the 30-bp promoter region around −169C→T evaluated by EMSA. Allelic difference and competition experiment (left) and supershift experiment using antibodies for NF-κB components (right). (**c**) Expression of *FCRL3* measured by quantitative TaqMan PCR of RNA purified from $CD19^+$ B cells obtained from 13 healthy volunteers (C/C, $n = 4$; C/T, $n = 5$; T/T, $n = 4$). (**d**) ASTQ. *FCRL3* transcripts in B cells and genomic DNA from individuals ($n = 5$) with heterozygous genotypes (−169C/T +358C/G) were amplified and quantified using an *EagI* restriction-fragment length polymorphism located at position +358. The 122-bp and 85-bp bands represent transcripts of the +358C allele and +358G allele, respectively. Transcripts from homozygous individuals (+358C/C and +358G/G) are shown as controls for digestion.

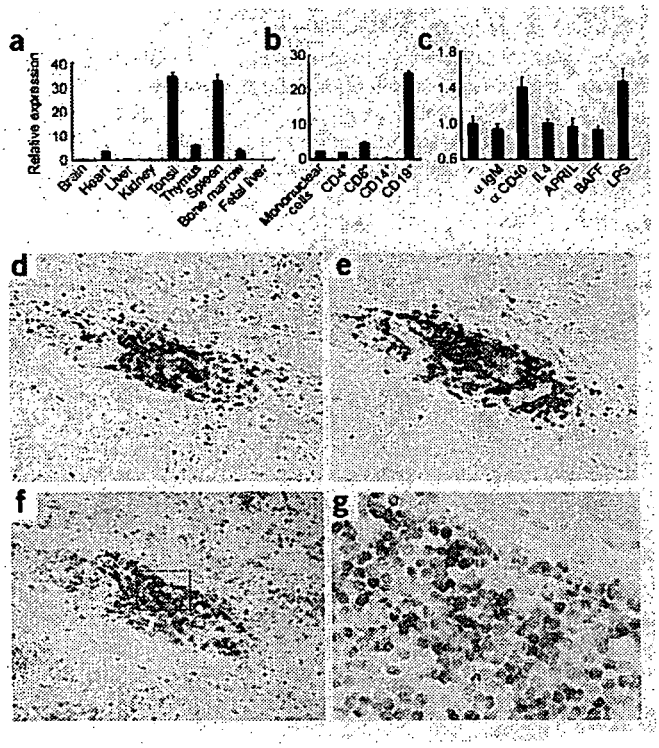

Figure 3 Expression patterns of *FCRL3* in human tissues and cells. (**a**) Relative expression of *FCRL3* in various tissues. (**b**) Relative expression of *FCRL3* in fractionated leukocytes using MTC panel (Clontech). (**c**) Relative expression of *FCRL3* in response to stimuli (antibody to CD40, 1 μg ml^{-1}; antibody to IgM, 1 μg ml^{-1}; IL-4, 10 ng ml^{-1}; APRIL, 10 ng ml^{-1}; BAFF, 10 ng ml^{-1}; LPS, 100 ng ml^{-1}) for 4 h. Representative data from three experiments done in triplicate. (**d**,**e**) Lymphocyte aggregates in rheumatoid arthritis synovium. T cells and B cells in serial sections were immunostained using antibodies to CD3 (**d**) and CD20 (**e**), respectively. (**f**,**g**) *FCRL3* mRNA expression (blue stain) in rheumatoid arthritis synovium as analyzed by *in situ* hybridization. Higher magnification views of synovium (**g**) are denoted by the box in **f** (magnifications: **d**–**f**, ×100; **g**, ×400). Counterstaining: **d**,**e**, hematoxylin; **f**,**g**, nuclear fast red.

oligonucleotides surrounding SNP −169C→T and control oligonucleotides into a vector with the SV40 promoter. Cells transfected with a single copy of the C allele produced substantially greater luciferase activity than cells transfected with a single copy of the T allele. More convincingly, transfection with four tandem copies of the C allele enhanced luciferase activity by a factor of 20 over transfection with four tandem copies of the T allele (**Fig. 2a**).

To elucidate specific nuclear factors that bind the disease-susceptible allele, we analyzed the sequence around −169C→T. These sequences were predicted by TRANSFAC software to have binding affinity for NF-κB, which regulates a wide variety of genes in the immune system. The disease-susceptible sequence (including −169C) had higher matrix similarity to the consensus NF-κB binding motif than the nonsusceptible sequence (including −169T). We then carried out electrophoretic mobility shift assays (EMSAs) to examine whether differences between the susceptible −169C allele and the nonsusceptible −169T allele affected binding of nuclear proteins from Raji cells. We used the same 30-bp labeled oligonucleotides used in the luciferase assay. These sequences contain the predicted NF-κB binding site. We observed two main bands, I and II, in the presence of nuclear extracts; the intensity of band I was higher for the susceptible −169C allele than for the nonsusceptible −169T allele (**Fig. 2b**). Competition assays with unlabeled oligonucleotides indicated that these complexes were specific for the probes. In addition, competition assays with unlabeled probes of the C allele for T and the T allele for C showed that the C allele was better able to compete for binding, a result consistent with the higher binding affinity of labeled C allele probes alone. We also carried out a supershift experiment with antibodies specific for NF-κB components (p50, p52, p65, RelB and cRel). We observed supershifts in some lanes with specific antibodies for p50, p65 and cRel (**Fig. 2b**). Among these, only antibody to p50 shifted band II, suggestive of the presence of a p50-p50 homodimer. Band I had the highest intensity and a substantial allelic difference and was supershifted by antibodies to p50, p65 and cRel. Although these findings indicate that band I comprises a mixture of heterodimers, the greater shifts caused by antibodies to p50 and cRel suggest that the main component is a p50-cRel heterodimer.

The two *in vitro* assays showed the potent transcriptional activity of the disease-susceptible haplotype regulated by NF-κB, suggesting that expression of *FCRL3* is greater from the disease-susceptible −169C allele than from the nonsusceptible −169T allele. To extend these findings, we quantified expression of *FCRL3* in peripheral blood B cells from healthy donors using quantitative TaqMan methods and analyzed the effect of the number of susceptible copies on the transcript level by regression model. Regression analysis identified a significant positive correlation between number of susceptible chromosomes and transcription level ($R^2 = 0.49$, $P = 0.0076$; **Fig. 2c**).

We also carried out allele-specific transcript quantification[9,34] to confirm the effect of the SNP on transcription. Using an *Eag*I restriction-fragment length polymorphism located at position +358 in exon 2 of *FCRL3* (fcrl3_5, +358C→G), we measured the relative contribution of each haplotype to transcript production in heterozygous individuals (**Fig. 2d**). We evaluated the transcripts of five doubly heterozygous individuals with genotype −169C/T +358C/G; the mean ratio (susceptible versus nonsusceptible haplotype) was 1.63, significantly higher than that of DNA amplicons (ratio = 1.06, $P < 1 \times 10^{-5}$) from the same individuals. (The quantity of template DNA from the two haplotypes was equal.) These results show that the

Table 3 Genotype and autoantibodies in individuals with rheumatoid arthritis

	RF		Antibody to CCP	
Genotype	*n*[a]	Serum level[b] (IU/ml)	*n*[c]	Positivity (%)
−169C/C	29	479.9 ± 91.3[d]	17	100.0[e]
−169C/T	75	323.7 ± 47.3[d]	35	94.3[e]
−169T/T	44	216.4 ± 44.0[d]	19	73.7[e]

[a]$N = 148$. [b]Mean ± s.e.m. [c]$N = 71$. [d]$R^2 = 0.049$, $P = 0.0065$ by regression analysis. [e]$P = 0.029$ by Fisher's exact test.